The Coastal-Tract (Part 2): Applications of Aggregated Modeling of Lower-order Coastal Change

Article *in* Journal of Coastal Research · February 2003

Source: OAI

CITATIONS
131

READS
407

12 authors, including:

Marcel Stive
Delft University of Technology
359 PUBLICATIONS **9,719** CITATIONS
SEE PROFILE

Alan Niedoroda
Wyndham Consultants, LLC
157 PUBLICATIONS **2,250** CITATIONS
SEE PROFILE

Huib de Vriend
178 PUBLICATIONS **8,018** CITATIONS
SEE PROFILE

Maarten Cornelis Buijsman
University of Southern Mississippi
78 PUBLICATIONS **2,327** CITATIONS
SEE PROFILE

Journal of Coastal Research	19	4	828–848	West Palm Beach, Florida	Fall 2003

The Coastal-Tract (Part 2): Applications of Aggregated Modeling of Lower-order Coastal Change

Peter J. Cowell[1], Marcel J.F. Stive[2,3], Alan W. Niedoroda[4], Don J.P. Swift[5], Huib J. de Vriend[3,9], Maarten C. Buijsman[6], Robert J. Nicholls[7], Peter S. Roy[1], George M. Kaminsky[6], Jelmer Cleveringa[8], Chris W. Reed[4], and Poppe L. de Boer[8]

[1]University of Sydney
Institute of Marine Science
NSW 2006, Australia

[2]Delft Hydraulics
PO Box 177, 2600 MH Delft
The Netherlands/Neth. Centre for Coastal Research (NCK)

[3]Department of Civil Engineering
Delft Univ. of Technology
PO Box 5048, 2600 GA Delft
The Netherlands

[4]URS Greiner Woodward-Clyde
USA

[5]Department of Ocean, Earth and Atmospheric Sciences
Old Dominion University
Virginia, USA

[6]Washington Department of Ecology
Coastal Monitoring & Analysis Program
Olympia,Washington, USA

[7]Flood Hazard Research Centre
Middlesex University
Queensway, Enfield,
EN3 4SF, UK

[8]Institute of Earth Sciences
University of Utrecht, 3508 TA Utrecht
The Netherlands

[9]University of Twente
PO Box 217, 7500 AE Enschede
The Netherlands

ABSTRACT

COWELL, P.J.; STIVE, M.J.F.; NIEDORODA, A.W.; SWIFT, D.J.P.; DE VRIEND, H.J.; BUIJSMAN, M.C.; NICHOLLS, R.J.; ROY, P.S.; KAMINSKY, G.M.; CLEVERINGA, J.; REED, C.W.; and DE BOER, P.L., 2003. The coastal-tract (part 2): Applications of aggregated modeling of low-order coastal change. *Journal of Coastal Research,* 19(4), 828–848. West Palm Beach (Florida), ISSN 0749-0208.

The *coastal-tract* approach to coastal morphodynamics, described in the companion paper (The Coastal-Tract Part 1), provides a framework for aggregation of process and spatial dimensions in modeling low-order coastal change (*i.e.,* evolution of the shoreline, continental shelf and coastal plain on time scales of 10^2 to 10^3 years). Behavior-oriented, coastal-change models encapsulate aggregate dynamics of the coastal tract. We apply these models in a coastal-tract framework to illustrate the use of the concept, and to explore low-order morphological coupling under different environmental settings. These settings are characterized by data-models that we have constructed from four contrasting continental margins (NW Europe, US Pacific, US Atlantic, and SE Australia).

The gross kinematics of the coastal tract are constrained and steered by sediment-mass continuity. The rate of coastal advance or retreat is determined quantitatively by the balance between the change in sediment accommodation-space, caused by sea-level movements, and sediment availability. If the lower shoreface is shallower than required for equilibrium (negative accommodation), then sand is transferred to the upper shoreface (NW Europe, US Pacific, and SE Australian cases modelled) so that the shoreline tends to advance seaward. This tendency also occurs when relative sea level is falling (coastal emergence). Coastal retreat occurs when the lower shoreface is too deep for equilibrium (positive shoreface accommodation). This sediment-sharing between the upper and lower shoreface is an internal coupling that governs first-order coastal change. The upper shoreface and backbarrier (lagoon, estuary or mainland) also are coupled in first-order coastal change. Sediment accommodation-space is generated in the backbarrier by sea-level rise (and reduced by sea-level fall), but the amount of space is also moderated by influx of fine sediments from the coast, or sand and mud from fluvial sources. Remaining space can then be occupied by sand transferred from the upper shoreface causing a retreat of the latter (transgressive phases modelled for NW Europe, US Atlantic, and SE Australian cases).

ADDITIONAL INDEX WORDS: *Aggregate change, shoreface, backbarrier, lagoon, scale, coastal tract, coastal-tract cascade, templating, data-model, behavior-oriented models, morphological coupling, sea level, sediment supply, coastal evolution, coastal management, sea-level rise, transgression, regression, barrier, continental-shelf, sediments, accommodation-space, numerical model.*

INTRODUCTION

In the companion paper, *Part 1* (COWELL *et al.*, 2003, this volume), we have described concepts of the *coastal tract, coastal-tract cascade* and *coastal-tract templating*. They provide a framework for modelling coastal morphodynamics on a wide range of scales (from seconds to millennia). We use these principles here (in Part 2), by reference to large-scale models and their application, to elucidate the aggregate-scale processes governing coastal-tract evolution. Further details can be obtained from earlier works describing these models (Table 1).

The paper is aimed also at demonstrating the common el-

03300G received and accepted in revision 10 July 2003.

ements of low-order coastal change. As outline in Part-1, low-order behavior entails coupling of the upper shoreface to both the backbarrier and the lower-shoreface (*i.e.,* continental shelf). Illustrations presented below draw from our comparative modeling of coasts from a wide range of settings in Australia, North America and Europe. In each case we have assumed alongshore homogeneity, so the illustrations do not deal with the more complicated cases involving heterogeneity referred to in Part 1. These were beyond the scope of our modeling so far and are the subject of ongoing research.

Scale and Forcing

Beyond the annual time scale in the coastal ocean, with rare exception more than enough power exists to entrain and transport sediment. Most transport involves to-and-fro displacements of sediments with very small net deposition or erosion. Measurable changes in coastal morphology results from these small net amounts accumulating over many years. Thus, prediction of processes acting over time scales of decades and longer entails the difficult task of resolving small net changes in a system characterized by large fluctuations (DE VRIEND, 1998, and 2003, this volume).

Because limited opportunity exists to measure environmental forcing in detail over such long periods, we must also rely on generalized representations of waves and currents, and assume applicability over long distances: *i.e.,* long-term change involves large length scales (Part 1). Figure 1a shows forcing scales ranging from individual storm events to changes in worldwide climate or sea level. The progression from event time scales ($< 10^0$ yrs) to millennia demands increasing generalization of theory and data, but generalization entails decreased resolution achievable from measurements and predictions (Figure 1a). Thus, *coastal-tract templating* procedures require an appreciation of coastal-change dependence on time-, and length-averaged quantities.

Changes that occur as the result of a single storm event can be studied in terms of the sediment movement brought about by a time series of waves, currents and water levels (sub-event scales $\leq 10^{-1}$ in Figure 1a). However, net morphological changes related to a sequence of storm and calm intervals tend to be less than those of each individual event so that analyses depending on summing individual event responses is prone to error. Thus, the sum of forcing-parameter variations may be characterized better as a statistical climatology. This allows the system response to be assessed in relation to the whole range of forcing conditions. Although this approach sidesteps the residual-error problem, the gain in reliability has a cost of reduced precision. That is, predictions based on such an approach can approximate average future conditions only, rather than individual realizations for a given sequence of events.

Representation of Aggregate Forcing

The large time scales relevant to the coastal-tract favor adoption of the highly aggregated approach to forcing embodied in *the sedimentation-regime* concept formalized by THORNE and SWIFT (1991) and THORNE *et al.* (1991) based on SLOSS (1962). The theory states that, over long time periods, the controls on coastal deposition are summarized by the so-called *Sloss variables* that include a) accommodation space available for deposition, b) sediment supply (rate and composition), and c) intensity of sediment transport. Variation (loss or gain) in accommodation space occurs due to changes in relative sea level. Sediment supply rates and composition (principally range of grain sizes) depend on deltaic, shelf and littoral sources and sinks outside the tract. The sediment-transport intensity governs sediment-dispersal mechanisms within a tract, but this third Sloss variable obviously also affects sediment supply.

Table 1. *Existing Large-Scale Behavior Models encapsulating principles of elements within the coastal tract. (CP = Cross-shore Profile. IDV = 1 Dimensional Vertical representation of depth-integrated sediment dynamics.)*

Acronym	Model Name	Type	Reference
ADM	Advection-Diffusion Model	CP model with 1DV macroscopic sediment dynamics	NIEDORODA *et al.* (1995)
HPM	Hinged Panel Model	CP model with 1DV input-filtered sediment dynamics	STIVE and DE VRIEND (1995)
STM	Shoreface Translation Model	CP model of morphokinematics	COWELL *et al.* (1995)
ASMITA	Aggregated Scale Morphological Interaction between a Tidal-inlet system and the Adjacent coast	Box model with spatially lumped, macroscopic sediment dynamics	BUIJSMAN (1997) STIVE *et al.* (1998)

The regime concept postulates that equations of state can be derived in terms of the Sloss variables. Thus, Sloss variables are macroscopic parameters that provide a highly aggregated (bulk) representation of conditions forcing the coastal tract. Various approaches related to this concept have been proposed (Figure 1a) such as *macroscopic forcing* (NIEDORODA *et al.,* 1995), *summary forcing* (STIVE and DEVRIEND 1995), and *abbreviated forcing* (COWELL *et al.*, 1995). In the first approach the forcing is reduced to time-, and space-averaged conditions which include a sediment-dispersal regime that reflects the general flow climatology and its variation across the continental shelf. In the second approach, the forcing is summarized according to key, representative conditions such as the power-equivalent wave and a long time-averaged current (*input filtering* of DE VRIEND *et al*., 1993). In the last approach, the forcing is abbreviated to a reduced set of Sloss variables: process parameters aggregated in terms of sediment *accommodation* space, sediment supply and morphological regime.

MODELS AND METHODS

The concept of the *coastal tract* emerged through our development of numerical models for long-term coastal processes (Table 1). These models compete and support each other by adopting different methods for aggregating coastal features and processes into sub-systems (*i.e.,* comprising the coastal tract). These models have one thing in common how-

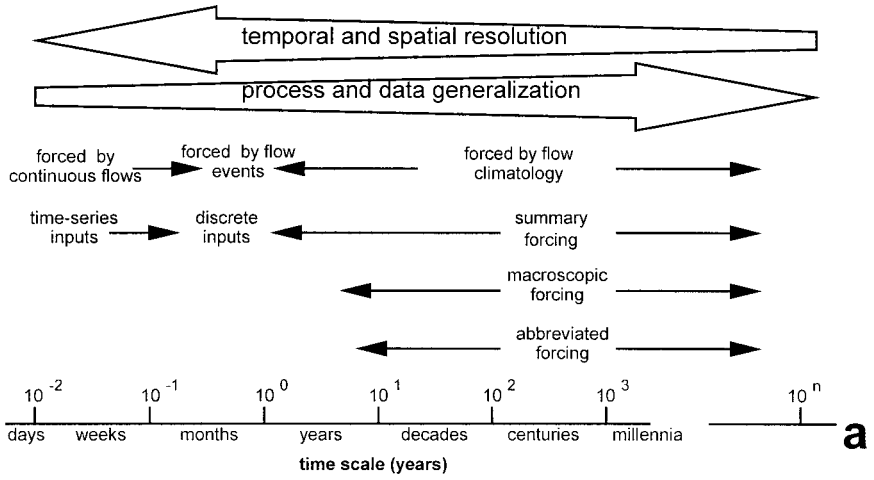

Model	Spatial Representation	Time Scale (years)	Forcing	Variables
Event	1-, 2-, or 3-D	10^{-2} - 10^{-1}	Direct/ continuous	Meteorological & Oceanographic
Event Sequence		10^{0} - 10^{1}	Direct/ Statistical	
ADM	Depth- & Width-Averaged	10^{2} - 10^{3}	Macroscopic	Sloss Variables
HPM			Summary	
STM			Abbreviated	Reduced Sloss Variables
ASMITA	System Averaged (non-spatial)		Summary	Sloss Variables
Hybrids	generally space averaged		as required	as required

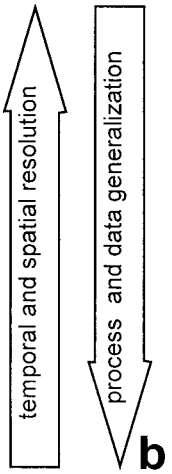

Figure 1. Scale and generalization in a) representation of *coastal-tract* forcing, and b) modeling framework for *coastal-tract* analyses.

ever: their sub systems share sediments and thereby interact dynamically (*morphological coupling*) on time scales of change related to size of sub systems. As part of the PACE project, the models were tested and compared, with the conclusion that each approach has contrasting strengths and weaknesses that collectively yield insights into coastal-tract behavior.

Scale and Process Representation: Comparative Modeling

Figure 1b summarizes the modeling approaches that can be applied to the coastal tract. Conceptually this summary extends Figure 1a by specifying the models with respect to their representation of forcing, governing variables and spatial dimensions.

Event-scale Models

Event-scale models are the smallest scale in the range, of which two types have been defined: a) *initial sedimentation/erosion* (ISE) models and b) *medium-term morphodynamic* (MTM) models (De Vriend *et al.*, 1993). Both include algorithms that provide computation of bed changes from sediment continuity based on transport fluxes driven by waves and currents. The ISE approach does not feed back the computed bed changes into another cycle of computation. Although useful as a diagnostic tool, the ISE approach cannot deal with long-term predictions involving successive morphology changes (*i.e.,* coastal evolution).

Models of the MTM variety are designed to cope with this problem. These models however can suffer from inadequately proscribed boundary conditions, numerical instabilities that promote growth of spurious morphological features, and un-

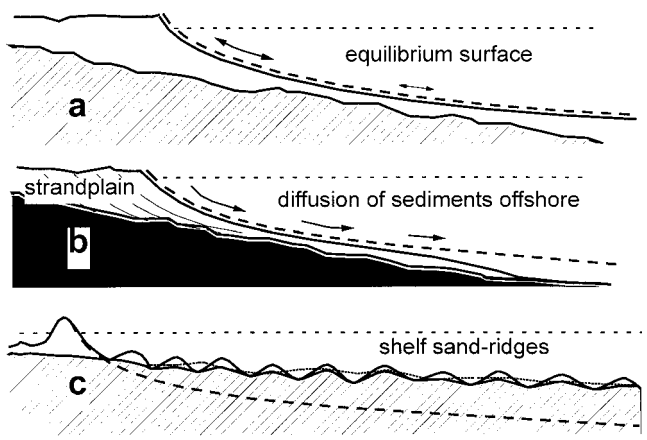

Figure 2. Inherited shelf slope compared to equilibrium shoreface after a period of sea-level stillstand and profile evolution: a) fully adjusted shoreface, b) shelf steeper than equilibrium shoreface providing sediment accommodation space offshore and deltaic sediment supply at the coast, and c) shelf much shallower than equilibrium shoreface causing negative accommodation space offshore.

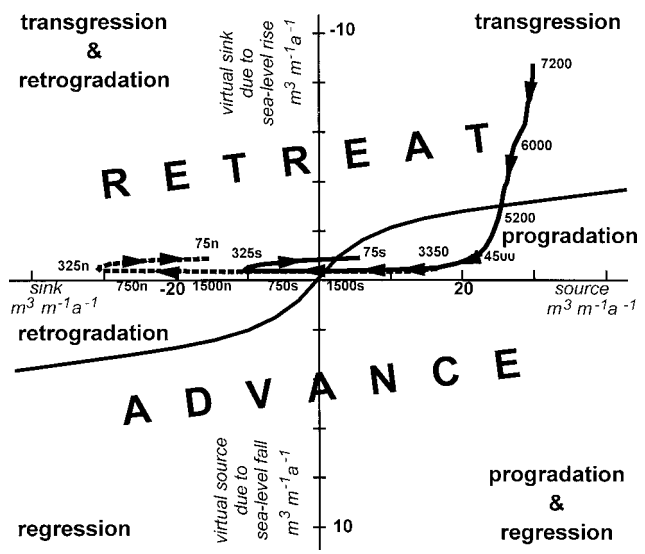

Figure 3. Evolution of the central Netherlands coast (Hoek of Holland to Den Helder) as a time trajectory in sediment-supply/accommodation phase space (abscissa and ordinate respectively, scaled in cubic meters per year per meter of shoreline). Numbers along the trajectory indicate time (years BP); suffixes n and s denote north and south of Haarlem respectively.

expected interactions between system components that cannot be anticipated from knowledge of how the separate parts behave in isolation (De Vriend *et al.*, 1993). Furthermore, there are difficulties in representing inputs (forcing and boundary conditions) over long periods of time. The problem has been addressed by reducing these inputs to statistical summaries (*e.g.,* Sherwood, 1995). Because most work is done by large storms however, it is presently not clear how to weight the statistical representation of inputs appropriately: the classical *magnitude-frequency* problem in geomorphology (Wolman and Miller, 1960). Even if these problems can be suppressed, the non-linearity of the large-scale processes must lead to progressive departures of predictions from real behavior: *i.e.,* because the latter is a time series of unique realizations (ensuing from a climatological history), whereas the former are merely estimates of central tendency for a system sensitive to initial conditions.

Nevertheless, event-scale modeling is useful as a diagnostic tool in coastal-tract modeling. It can be applied with large-scale models that require internal calibration and estimates for boundary conditions. That is, synthetic data computed from event-scale models can be used to supplement incomplete field-data sets if adequate representation of the physics exist for the small-scale processes; and these may well include subtle but important effects such as bed armouring, wave-ripple effects, and 'lidding' of the wave boundary layer (Reed *et al.,* 1999).

Aggregate-scale Models

For long-term predictions, we can by-pass the problem of having to predict and time-integrate very small differences in highly variable systems. This is achieved by deriving macroscopic variables (*e.g.,* Sloss variables) that define the physics directly on the scale of interest. For these systems, ISE processes simply become noise, although estimates of them inform us about the intensity of sedimentation regime.

Our physical concepts of the *coastal tract* derive significantly from ideas underlying the Sloss variables. Accommodation space can be either positive (under-filled) or negative (over-filled) and commonly varies spatially over the profile (Figure 3 in Part 1). The concept applies equally to the volume created on a shelf (Figure 2) or within an estuary by sea-level rise that exceeds the sedimentation rate. Available hydrodynamic power controls the rate of morphological change. Characterization of the power changes according to the system, but generally takes some form of aggregated wave- or flow-climatology. The grain size and supply rate of sediment are usually externally controlled. The detail at which these are quantified depends on the nature of the coastal-tract system under investigation.

Large-scale models shown on Figure 1b utilize the Sloss-variables, but in different ways (see Table 1 for acronyms, details and documentation). The HPM incorporates all the Sloss-variables: translation of the form-invariant upper shoreface occurs in response to interaction between sediment supply and changes in accommodation space due to sea-level variations. Depth-averaged variables representing the power-equivalent wave and current environment govern sediment transfer between hinged panels that characterize the lower, middle and upper shoreface (Stive and De Vriend, 1995).

The ADM also contains the Sloss variables although it does not employ representative hydrodynamic power in transporting sediments. Rather, the model aggregates transport events into macroscopic processes (advection and diffusion) that are calibrated against measures of hydrodynamic power for specific sites (Carey *et al.*, 1999). Again there is an interaction

between sediment supply (positive or negative) and sea-level related change in accommodation space, with responses governed by the advection-diffusion processes.

The STM operates with a reduced set of Sloss variables since the hydrodynamic forcing is expressed through morphological regime: *i.e.,* sediment-transport intensity represented implicitly via coastal-profile geometry that varies through time with forcing parameters. Geometries for the upper shoreface, lower shoreface, and backbarrier are calibrated against field data, including radiometrically measured morphological history and hindcastings of associated wave and tide regimes, using empirical relations and other event-scale models (COWELL *et al.*, 1999b, 2003). The balance between changes in process-related profile geometry, accommodation-space (due to changes in sea level), and sediment supply governs profile kinematics.

ASMITA bears a similarity to the panel model and also the ESTMORF model for tidal basins (WANG *et al.*, 1996). Accommodation-space is represented by a series of control volumes (or panel elements) for the shoreface, ebb- and flood-tide deltas, tidal-inlet channel, and tidal-basin channel-network. Morphodynamic change in each element is specified by time-averaged physics that are related to the Sloss variables. An equilibrium system is developed and then perturbed to study the responses of the system elements and the interaction between these elements.

Comparative tests revealed different strengths and weaknesses among these models. Work in progress thus aims to combine the individual modeling approaches and the models themselves. An example is the nested ASMITA-ADM hybrid (see Figure 12 further on) that simulates lagoon-shoreface coupling over space and time scales not possible using either model alone.

Data-Model Templating

Coastal-tract delineation for a site specific case requires development of a *data-model* that aggregates process and morphological properties as they exist in nature (Part 1). Application of numerical models and empirical analyses to predict site-specific, low-order, coastal change both require a data-model before prediction can proceed. The data-model links the process model to that part of nature represented in the process model. Such a linkage is necessary to calibrate the process model and to assess its results.

Generally, data-model development occurs intuitively without explicit recognition as a formal step in coastal research. The risk here is that ambiguities occur during analysis, modeling and interpretation of results, introducing additional uncertainty into coastal-change prediction, as well as tensions between practitioners of data-driven and model-driven approaches to large-scale coastal behavior (*cf.,* PILKEY, 1993). The coastal-tract concept therefore seeks to formalize procedures for linking coasts in nature to models that have much lower dimensionality: *i.e., templating*.

First-order change in the coastal tract is constrained by the environmental setting: *i.e.,* zero-order in the tract-cascade (Part 1). The environmental setting depends mainly upon sediment supply and steepness of the continental shelf and the hinterland (Figure 2). The shelf steepness determines how far the shoreface was from equilibrium at the onset of sea-level stillstand (or near stillstand) at the end of the post-glacial marine transgression (5 to 6 ka BP). Steeper shelves and hinterlands are more likely to have shorefaces that are too deep to be in equilibrium for a given coastal-ocean climatology and endemic sediment sizes (Figure 2b). Backshores under these conditions are more likely to be a mainland beach than a barrier lagoon (see Figure 1b in Part 1). Parts of the southeast Australian coast (ROY *et al.*, 1994) and much of the Pacific US coast (KAMINSKY *et al.*, 1997) have this type of setting.

The converse is true for low gradient shelves and hinterlands where a) the shelf surface is more likely to be shallower than the equilibrium shoreface, and b) the backshore is more likely to comprise a lagoon, in-filled to some degree depending on sediment supply (Figure 2c). The coasts of eastern USA (SWIFT, 1976) and northwest Europe (BEETS *et al.*, 1992) are examples. The stage of coastal evolution therefore depends on a) how far the shoreface was from equilibrium at the end of the post-glacial marine transgression, b) the size of the lagoon at that time, and c) the sediment supply since then.

COASTAL-TRACT MODELING

Description of our comparative modeling provides a vehicle to elucidate the general principles outlined in Part 1 regarding coastal-tract behavior. This objective is enhanced because the modeling exploited data sets from a wide range of environments, allowing us to study low-order change under contrasting conditions.

The coastal-tract principles are not entirely new: they were implicit in earlier kinematic models for first approximation of long-term coastal change, and in related ideas. In a narrow sense, the Bruun Rule is an upper-shoreface response to a reduced set of Sloss variables, that include sea-level rise and sediment supply, with the response involving sand transfers between the shoreface and the backshore or backbarrier (DEAN and MAURMEYER, 1983). In a broader sense, SWIFT (1976) extended CURRAY's (1964) ideas into a general framework for long-term coastal change entailing *transgression* (landward retreat) and *regression* (seaward advance) of the shoreline due to sea-level rise and fall, with corresponding tendencies toward *retrogradation* and *progradation* due to net sediment losses or inputs alongshore.

Overall therefore, the kinematics of the coastal tract schematized by Figure 3 in Part 1 are constrained and steered by sediment-mass continuity in response to the Sloss variables. We consider the general kinematics formally in the following section, after which we examine more specific modes of tract behavior. The examination proceeds within the coastal-tract framework (Part 1) through application of computer models to morphostratigraphic data sets (identified in Tables 1 and 2 respectively).

Gross Coastal Tract Kinematics

SWIFT's (1976) concepts can be quantified in the context of the coastal tract, and related back to the familiar *Bruun Rule*

Table 2. *Morphological and stratigraphic data sets used in comparative modeling and illustration of aggregated processes within the coastal tract, and their locations.*

Data Set	Comparative Properties	Summary Reference
Netherlands: Haarlem, Central Holland	Closed barrier (inlet-free) coast with low-gradient shelf and low (−ve) sediment input	BEETS, *et al.,* 1992; STIVE and DE VRIEND, 1975
Netherlands: Terschelling, Wadden Friesland	Barrier-inlet tidal basin coast with lo-gradient shelf and low (+ve) sediment input	SHA, 1992; VAN DER SPEK, 1994
SE Australia: Tuncurry Bay	Closed barrier (inlet-free) coast with steep shelf and low (+ve) sediment input	ROY *et al.,* 1994, 1997
NW USA: Columbia River coastal cell (Tillamook Head to Point Grenville)	Mixed closed and barrier-inlet coast with steep shelf and moderate (+ve) sediment input	STERNBERG, 1986; PETERSON and PHIPPS, 1992; WOLF *et al.,* 1997; KAMINSKY *et al.,* 1997
E. USA: Duck NC	Mixed closed and barrier-inlet coast with steep shelf and sediment input during post glacial transgression	FIELD *et al.,* 1979; MEISBURGER *et al.,* 1989

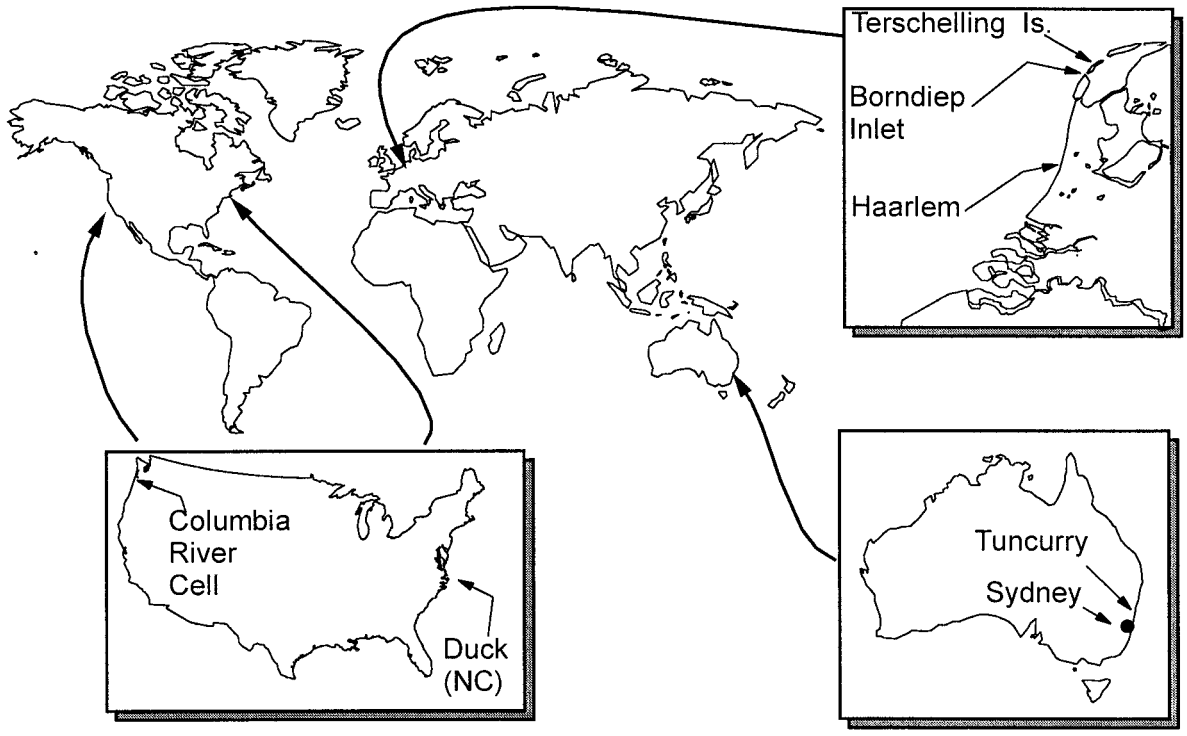

(BRUUN, 1962), if we consider the sediment balance of the upper shoreface. We adopt the assumption that the upper shoreface to a first approximation is form invariant relative to mean sea-level over time periods ($\gg$1 yr) for which profile closure occurs (NICHOLLS *et al.*, 1998). We can represent the upper shoreface by an arbitrary, but usually concave-up, profile $h(x)$ to a depth h_* and a length L_*, in which x is the distance from the shore (DEAN, 1991). Sediment-volume conservation for profile kinematics requires that

$$\frac{\partial h}{\partial t} + c_p \frac{\partial h}{\partial x} = 0 \tag{1}$$

or via $h = MSL - z_b$

$$\frac{\partial z_b}{\partial t} + c_p \frac{\partial z_b}{\partial x} = \frac{\partial MSL}{\partial t} \tag{2}$$

where c_p is the horizontal translation rate of the shoreline position. The sediment-transport balance equation for a fixed spatial control volume is

$$\frac{\partial z_b}{\partial t} + \frac{\partial q_x}{\partial x} + \frac{\partial q_y}{\partial y} + s = 0 \tag{3}$$

where $q_{x,y}$ are the cross-shore and alongshore sediment transports, and s is a local source or sink. These equations may be combined to yield

$$c_p = \frac{\partial MSL}{\partial t}\left(\frac{\partial h}{\partial x}\right)^{-1} - \frac{\partial q_x}{\partial h} - \frac{\partial q_y}{\partial y}\left(\frac{\partial h}{\partial x}\right)^{-1} - s\left(\frac{\partial h}{\partial x}\right)^{-1} \tag{4}$$

or, after cross-shore integration over L_*,

$$c_p h_* = \frac{\partial MSL}{\partial t} L_* - (q_{x,sea} - q_{x,dune}) - \frac{\partial Q_y}{\partial y} - s \tag{5}$$

in which Q_y is the alongshore transport integrated over L_*.

In the absence of littoral transport gradients and other

sources or sinks (including sand exchanges with the lower shoreface and backbarrier) the above reduces to the standard *Bruun Rule* (BRUUN, 1962):

$$c_p = \frac{\partial MSL}{\partial t}\left(\frac{L_*}{h_*}\right) \quad (6)$$

Equation 5 is similar to the DEAN and MAURMEYER (1983) version of the Bruun Rule, an analytical precursor of the coastal-tract concept. The shoreline-change rate is determined quantitatively by the balance between the 'sink' term, for accommodation-space generated due to sea-level rise (first term on the right-hand side), and sediment availability (being the sum of sinks and sources, the last three terms on the right-hand side of equation 5). The relative sea-level change is a virtual sink/source term since there is no absolute loss, although the response is comparable to the impact of a real source/sink regarding horizontal movements of the upper shoreface.

The source and sink terms in equation 5 allow the qualitative Curray-Swift model of coastal evolution to be quantified as a time trajectory in sediment source/sink phase space: *e.g.,* evolution of the well-documented central Netherlands coast between Hoek of Holland and Den Helder in Figure 3. The trajectory is based on a) estimates derived from radiometric data by BEETS *et al.* (1992), listed in the Annex, for the period 5000–0 years BP; and b) the results of STM simulations for 7200–5000 BP. The line separating advance and retreat of the coast is fitted for the trajectory in the top-right quadrant, with its mirror image assumed for the bottom-left quadrant in the absence of other data. The trajectory bifurcates after 2000 BP because differences develop in rates of shoreline change averaged alongshore north and south of Haarlem (see Table 2 for location). The shape of the advance/retreat-threshold curve demonstrates that coastal evolution is governed mainly by a) sediment supply ($\pm$) under near-stillstand sea-level conditions (such as those predominating in the late Holocene), and b) change in accommodation space when sea-level changes rapidly (such as during global glaciation and deglaciation).

Low-order Shoreface Processes

Dynamics

We depart from conventional definitions of the shoreface which, as a component of the coastal tract, we regard ostensibly as comprising the entire sub-aqueous continental-shelf surface (Part 1). We assume that the main flows responsible for shore-normal sediment fluxes on the shoreface comprise wind waves and swell, wind-driven flows (upwelling and downwelling), tidal currents (especially in the vicinity of estuaries), and surf-zone flows (especially undertow) on the upper shoreface (NIEDORODA and SWIFT, 1991; STIVE *et al.*, 1991; WRIGHT, 1995; COWELL *et al.*, 1999a). On time scales relevant to coastal-tract behavior, aggregate sediment dynamics respond to a coastal-flow climatology that can be characterised only as a magnitude-frequency distribution.

The effects of wind-wave and swell asymmetry in this climatology can be thought of as advecting sediments onshore, if we assume that residual wave transports act only in the shoreward direction. Other components of the flow climatology drive sediments onshore and offshore through irregular cycles of varying amplitude and periodicity, such that net fluxes behave diffusively. In aggregate, these sediment dynamics are analogous to large-scale turbulence in which horizontal eddy diffusion characterizes across-shore sediment dispersal, with the length scale of the eddies increasing with distance from shore. This concept of macroscopic sediment dynamics was introduced by NIEDORODA *et al.* (1995) who represented the time-averaged across-shore transport-volume flux as

$$Q_x = q_{x,ad} + q_{x,dif} + q_{x,g} + s_x \quad (7)$$

for each point along the shoreface profile at a positive distance x from the shore, where subscripts *ad, dif,* and g denote advection, diffusion, and gravity respectively, while s is a source or sink effect due to net along-shelf transports at any point.

The first term on the right in equation 7 captures the advective effect of wave asymmetry on sand transport. This term is a lumped representation of the depth-dependent sediment flux, due to combined wave- and current-driven transports and effects related to bottom slope. Onshore directed wave-asymmetry effects dominate on shallower parts of the shoreface. The second term represents the long-term depth-averaged total-load transport, the behavior of which is controlled in aggregate by an average-annual horizontal diffusion coefficient (that is also depth dependent) and the cross-shore gradient of the representative sediment concentration (a depth dependent variable).

The concept underlies the Advection-Diffusion Model (ADM in Table 1) which expresses the long-term sediment-transport regime associated with a site-specific coastal-ocean climatology. The ADM assumes that coastal-tract morphology is shaped by space- and time-averaged processes. The ADM *data-model* thus requires elimination of local relief through spatial-averaging over several kilometers along the cross-shore profile. Usually a sediment input (or loss) at the shoreward end of the profile is set to represent the average rate of terrestrial input per unit coast length, but sediment can also be directed into the model offshore, as would occur from alongshelf-transport gradients. The hydrodynamic and diffusion parameters are fitted by successive trials until a uniformly bypassing profile of the correct shape is obtained. An actual sea level history is then used to drive the evolution of the profile.

The aggregate processes represented in equation 7 are illustrated in the modeling of the Columbia River coastal tract (Table 2) using the ADM (Table 1). Essentials of the data-model (Figure 4a) include an aggraded shoreface overlying an erosion surface dating from 7000 years BP (WOLF *et al.*, 1997), and a prograded strandplain, interrupted by inlets to barrier lagoons (KAMINSKY *et al.*, 1997). In reality the ocean floor beyond the continental shelf lies at depths larger than 1200 m but, for practical reasons, the data-model ocean floor lies at about 300 m (which has only minor influence on the ADM calculations). The external forcing includes sea-level rise, and a sediment supply from the Columbia River estimated to total 17.5 million m^3a^{-1}, with sediment losses be-

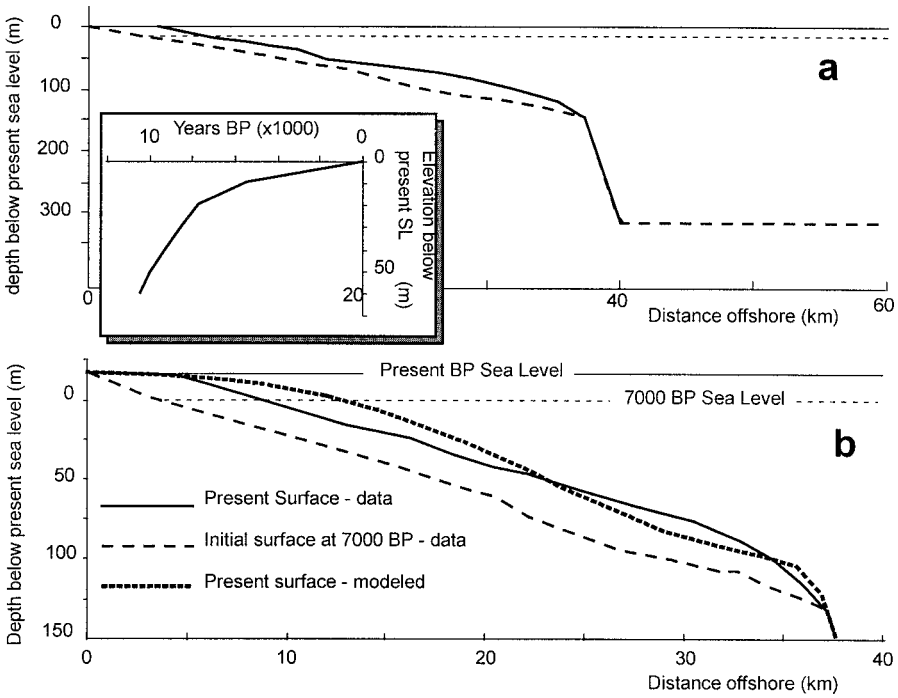

Figure 4. Columbia River coastal-tract: a) Data-model for the including initial surface (dashed) dating from 7000 years BP beneath the present surface (solid line) with sea-level curve (inset); and b) ADM simulation of Columbia River coastal-tract evolution from 7000 BP to present.

yond the continental-shelf edge (STERNBERG, 1986) and to the backbarrier tidal basins estimated at 0.7 and 2.4 m^3a^{-1} respectively. The result is a net sediment input of 14.4 million m^3a^{-1}, averaged over the approximately 150 km alongshore distance characterized by the Columbia-River tract. Since the shoreface of the Columbia tract has experienced net aggradation during the past 7000 years, the initial shoreface was necessarily deeper than equilibrium, providing positive sediment-accommodation space on the shelf (*cf.* Figure 2b).

Modeled offshore diffusion of sediments supplied at the coast by the Columbia River give a net accreted volume close to the measured volume of post 7000 BP deposition on the shoreface totalled out to the shelf edge (Figure 4b). Although the results indicate that diffusion rates in nature are higher than those used in the model, the discrepancy may be due to limited viability of the alongshelf-homogeneity assumption for the Columbia shoreface: *i.e.,* fine-sediment deposits occur in field data as a distinct band trending diagonally across the shelf (STERNBERG, 1986). Nevertheless, the ADM results overall are consistent with the data-model. Both indicate that diffusion is incapable of displacing all sediments to the lower shoreface. Thus, the rate of sediment supply at the coast by the Columbia together with the onshore advection due to waves resulted in simulated progradation of the upper shoreface in addition to overall aggradation of the lower shoreface (Figure 4b).

The advection-diffusion processes are continuous across the entire shoreface, but the terms in equation 7 and the balance between them varies systematically with water depth and distance from the coast. Thus, the advective effects offset the diffusive effects to the greatest degree in shallow water. The variation in relative importance of these effects across the shoreface (*i.e.,* first two terms in equation 7) forms the basis of the separate but coupled behavior of the upper and lower shoreface.

Upper-lower Shoreface Coupling

In shallower depths on the shoreface, the enhanced effect of shoreward sediment advection (first term in equation 7) can overwhelm the seaward-acting diffusion effects. The Hinged-Panel Model (HPM in Table 1) represents advective processes involving BOWEN's (1980) version of Bagnold's *energetics* transport model, with the seaward-directed diffusive effects simply represented by downslope gravity. The HPM was developed to analyze a shore-normal profile extending from the surf zone to the lower shoreface on an open ocean coast with uniform alongshore bathymetry. The profile is portrayed as discrete sections (panels) representing the upper, middle and lower shoreface. The profile of the upper shoreface is assumed to keep its shape while translating on-, or offshore. The sediment transfer between panels is computed from width-, and depth-averaged variables representing the power-equivalent wave and current environment. Profile changes are constrained by sediment mass conservation.

Central Netherlands: Haarlem. Application of the HPM to the Holland coastal tract demonstrated the combined effect of an external littoral supply of sediments to the tract and the transfer of sand from the lower to the upper shoreface within the tract (STIVE and DE VRIEND, 1995). The data-

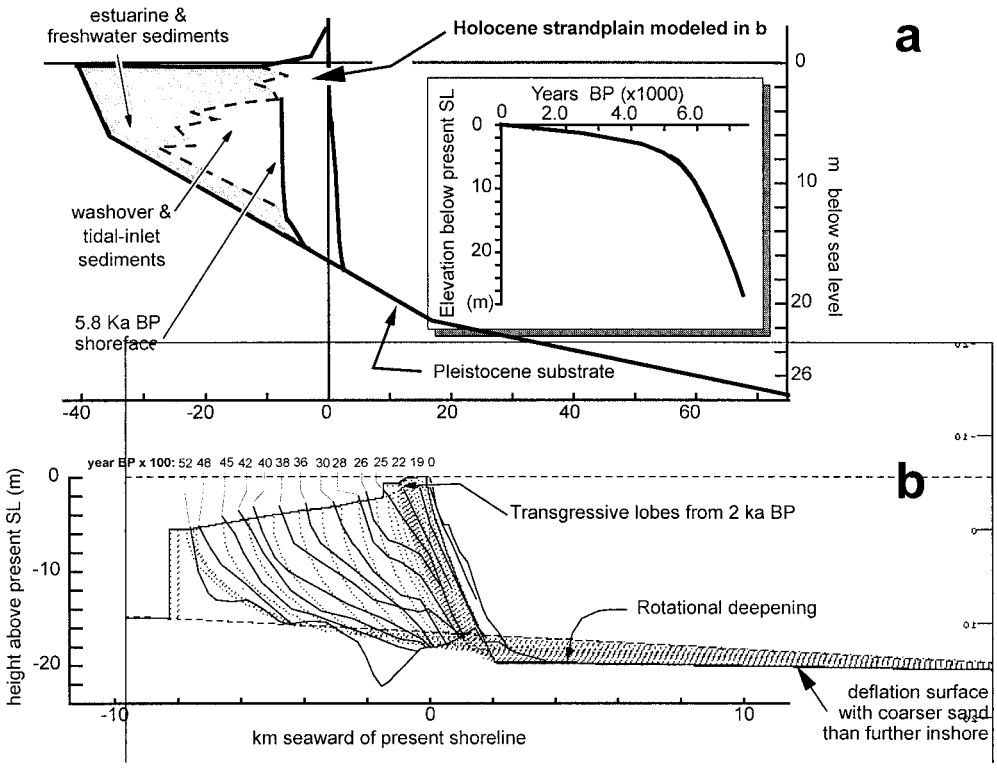

Figure 5. Seaward translation of the upper shoreface in the Holland coastal tract driven by littoral sediment feed and a deepening of the landward 10 km of the lower shoreface, with the deepening decreasing progressively in the offshore direction: a) data-model; and b) STM simulation overlaid on data-model isochrons (solid lines). The steeply dipping dotted lines within the strandplain depict positions of the STM shoreface during previous time steps: i.e., synthetic isochrons. The dotted lines on the lower shoreface are earlier erosion surfaces.

model was based on morphostratigraphic surveys calibrated by radiocarbon dates from a strandplain that formed along the full length (100 km) of the cell after about 5000 BP, when inlets to the tidal basin closed (BEETS *et al.*, 1992; VAN DER VALK, 1992). The data-model comprises a gently sloping lower shoreface (Figure 5a) indicative of a negative accommodation capacity offshore (Figure 2c), a strandplain volume estimated at some 6×10^6 m^3 supplied between 5000 and 2000 BP, with less than half the amount thought to be supplied from adjacent coastal tracts (BEETS *et al.*, 1992). The remainder is thought to have been reworked from the shoreface, primarily from the subaqueous tidal deltas but also from the landward segment of the lower shoreface.

STIVE and DE VRIEND (1995) used the HPM to simulate these processes. The kinematics are reproduced in Figure 5b using the Shoreface Translation Model (STM in Table 1) applied to the same data-model, beginning with a littoral feed of 30 m^3 a^{-1} per meter of coastline from 5200 to 3600 BP, then declining by 5 m^3 a^{-1} m^{-1} until 2000 BP when it was stabilized at -0.5 m^3 a^{-1} m^{-1}. The cross-shore transfer of sand to the upper shoreface was modeled by adjusting profile geometry through time. More specifically, a deepening of the upper-lower shoreface boundary in the STM (L_* in equation 5) was imposed at a rate of 0.17 m per 100 years consistent with, although less than, rates of measured bathymetric change (STIVE *et al.*, 1991; HINTON *et al.*, 1999). The lower shoreface deepening extended 10 km seawards at rates that decreased linearly with distance. The simulated process (Figure 5b) provided 49 percent of the strandplain volume.

These results suggest that the coupling between the upper and lower shoreface on the Holland coast is an important factor offsetting tendencies toward shoreline recession due to littoral sand losses from the tract. This stabilizing form of low-order coastal behavior has been overlooked in coastal-management studies in general (COWELL *et al.*, 2003). Nevertheless, each of our data sets (Table 2) contains evidence for this type of behavior. For example a coarse sediment lag exists on the lower shoreface at each of the field sites, and such deposits are widespread elsewhere throughout the world (COWELL *et al.*, 1999a, 1999b, 2003), indicative of surface lowering.

SE Australia: Tuncurry. Amongst the first descriptions of coarse sediments on the lower shoreface came from the Holland coast (VAN STRAATEN, 1965). They have been analyzed in detail for the Tuncurry site in SE Australia (Table 2) regarding their relationship to the underlying parent material from which they were shown to derive (ROY *et al.*, 1997). Typical of SE Australia, the lag deposits occur in water depths greater than roughly 20 m and extend as a shore-parallel band up to 10 km in width (ROY *et al.*, 1994).

Simulation of the Tuncurry-strandplain formation using the STM (Figure 6) illustrates genesis of the lag deposits

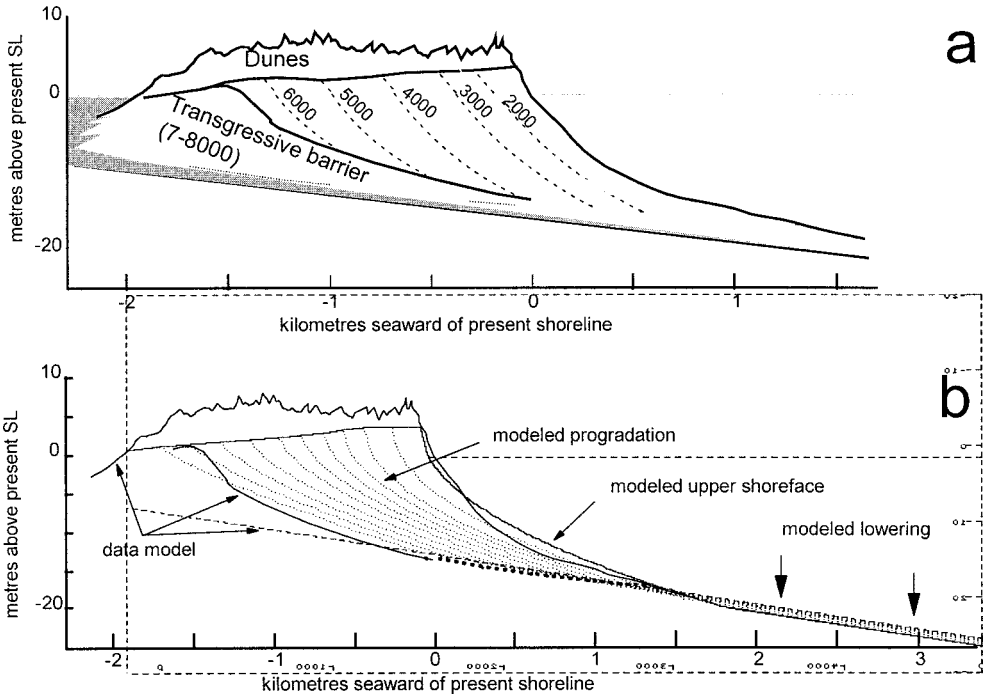

Figure 6. Tuncurry coastal tract, SE Australia: a) data-model based on radiometric dating of cores samples and ground-penetrating radar, with the isochrons labelled in years BP (ROY *et al.*, 1997); and b) STM simulation output overlaid on data-model.

through low-order behavior similar to that evident on the Holland coast. The Tuncurry coastal tract characterizes a cell spanning 11.5 km of coastline in which progradation has averaged 0.3 m a^{-1} throughout the Holocene (Fig 6a). The simulation involved a constant sea level for 6000 years, a progressive increase in runup elevation from 1.5 to 4.0 m above MSL due to increasing wave exposure, a steady increase in the depth of the upper-lower shoreface boundary at a rate of 0.002 m per year, decreasing linearly with distance for 10 km across the lower shoreface, and a constant littoral sand feed of 0.25 m^3 per year per meter of shoreline (Figure 6b). Sand supply from the lower to the upper shoreface due to shoreface deepening averaged 1.1 $m^3\ a^{-1}\ m^{-1}$ over the 6000 year period, thus supplying 80 percent of the sand comprising the prograding strandplain. The sand transfer is well below detection and prediction limits on annual time scales. Nevertheless, such small net residuals aggregate to produce all of the mean trend behavior within the Tuncurry coastal tract.

NW USA: Columbia River Coast. The Columbia River coastal tract (Table 2) provides a particularly valuable opportunity to substantiate Haarlem-Tuncurry type coupling between the upper and lower shoreface. Cycles of earthquake-induced subsidence and subsequent rebound occur at roughly 500 year intervals in the NW Pacific coastal region (KAMINSKY *et al.*, 1997). These tectonic processes cause episodes of sudden rise in relative sea levels, estimated at roughly 1–2 m, followed by gradual isostatic re-emergence. Responses to these events are evident in heavy mineral seams and shore-parallel lineaments in dunes within the strandplains (MEYERS *et al.*, 1996; KAMINSKY *et al.*, 1997). The data-model (Figure 7a) used with simulations was described in connection with Figure 7a, but for the shoreface coupling experiments the data-model also incorporates surface morphology generalized from the Long Beach strandplain, and a sea-level curve in which the magnitude of subsidence events is proportional to the duration between them based on marsh data (ATWATER *et al.*, 1995).

The results of the Columbia simulation show that it is impossible to reproduce present shoreface morphology without progressive deepening of the lower shoreface. Under conditions of earthquake induced sea-level fluctuations simulated with a time-invariant shoreface in the STM, the prograding sediment wedge produced a pronounced bulge in the shoreface (Figure 7b) that is absent from the data-model (Figure 7a). The sand contained within the submarine bulge reduces the sub-aerial volume so that progradation of the simulated strandplain is significantly less than in the data-model.

Simulation of time-varying shoreface responses to sudden sea-level rise using the STM involved reducing water depth (h_*) at the upper-lower shoreface boundary from 20 m to 15 m upon the occurrence of a subsidence event. Gradual shoreface deepening during the subsequent period of gradual rebound was simulated by increasing h_* at a rate of 0.01 m per year, reducing progressively to zero 2000 m further seaward (Figure 7c). The effect of shoreface deepening was to subdue the submarine bulge in the prograding sand wedge. In time steps immediately following an earthquake, the effect involved transfer of sand seaward. The aggregate effect however over a full subsidence-rebound cycle was net displacement of sediment to the sub-aerial portion of the prograding

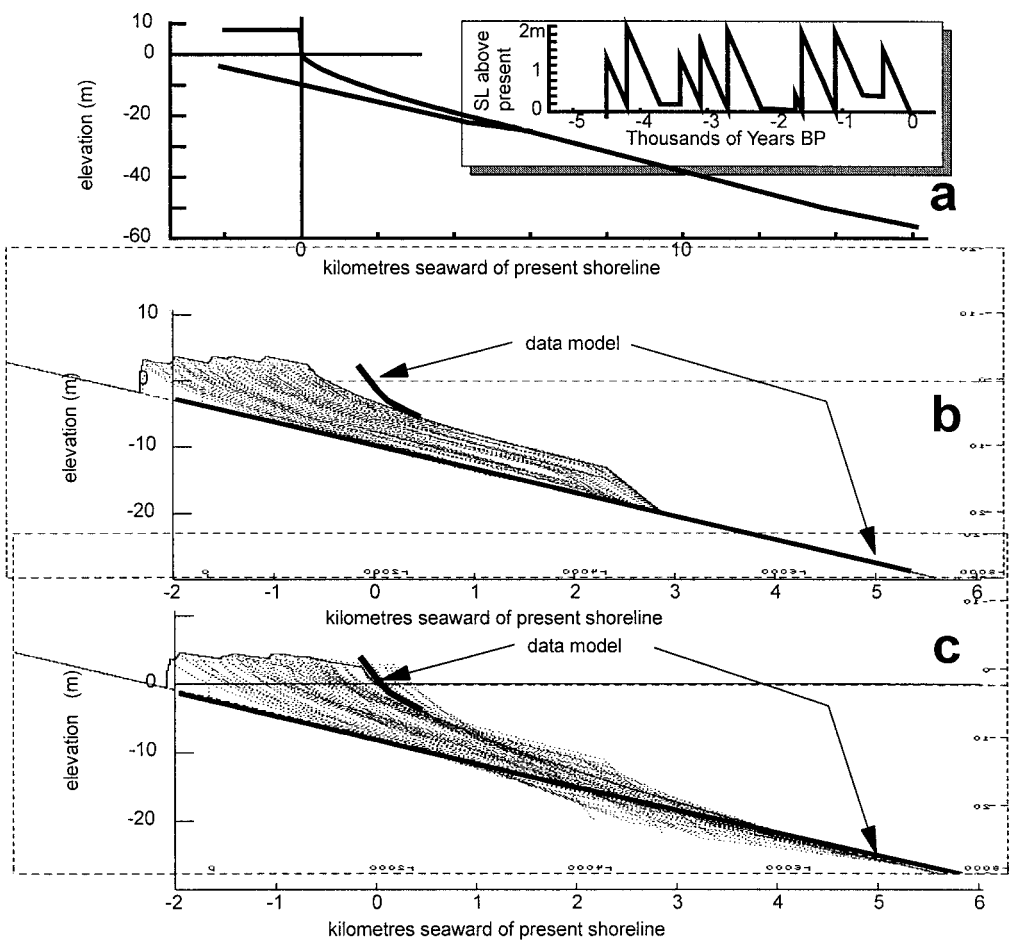

Figure 7. Columbia coastal tract, SW Washington, USA subject to seismically induced sea-level variations and littoral sediment feed: a) data-model, b) STM simulation without shoreface deepening, and c) STM simulation with shoreface deepening between earthquake events.

sand wedge. The simulated wedge is geometrically consistent with the data-model.

Falling Sea Level. A similar requirement for coupling between the upper and lower shoreface exists during falling sea levels in general. Since we assume that the upper shoreface can attain an equilibrium on the decadal time scale (ie., it has invariant time-averaged form extending seaward to a time-scale dependent closure depth), then the toe of the upper shoreface descends at the same rate as the falling sea level. The lower shoreface however must also degrade so that its elevation remains less than that of the upper shoreface. Otherwise a shear-stress shadow zone would form if the water depths increased further inshore, as would occur in the absence of coupling. Thus, as in the previous examples (Figures 4 to 6), a coupling exists involving a deepening of the landward portion of the lower shoreface with a corresponding transfer of sediment from the lower to the upper shoreface constrained by mass-conservation. The consequence is a prograding strandplain (COWELL *et al.*, 1999b).

Our Tuncurry data set (Figure 8a) contains stratigraphic evidence of shoreface behavior as sea level fell through tens of meters during the onset of the last glacial period 50–30 thousand years ago. Sea-level estimates were derived from uplifted coral terraces in New Guinea (CHAPPELL and POLACH, 1991). Strandplains developed in response to falling sea levels and are now located in 30–80 meters of water off the present coast. Seismic data and thermoluminescence dates from cores through the strandplains show that pre-existing sediments comprising the substrate were eroded to depths greater than 15 m below the present seabed, and subsequently backfilled with upper-shoreface sediment to produce the strandplains (ROY *et al.*, 1997).

At least two phases of strandplain development occurred, as indicated by the formation of backbarrier lagoonal deposits midway along the sequence (about 11 km offshore from the present coast in Figure 8a). These distinct phases correlate with the fluctuations in the overall trend of falling sea level (Figure 8a inset). The fluctuations were ignored however in STM simulations: only sea-level trends apply. Figures 8b and 8c show the STM simulation of strandplain formation after sea level had fallen continuously through 80 m. During this process, deepening of the lower shoreface was imposed in the simulation to a distance of 10 km seaward of the upper shoreface (*i.e.,* the active width of the lower shoreface specified in

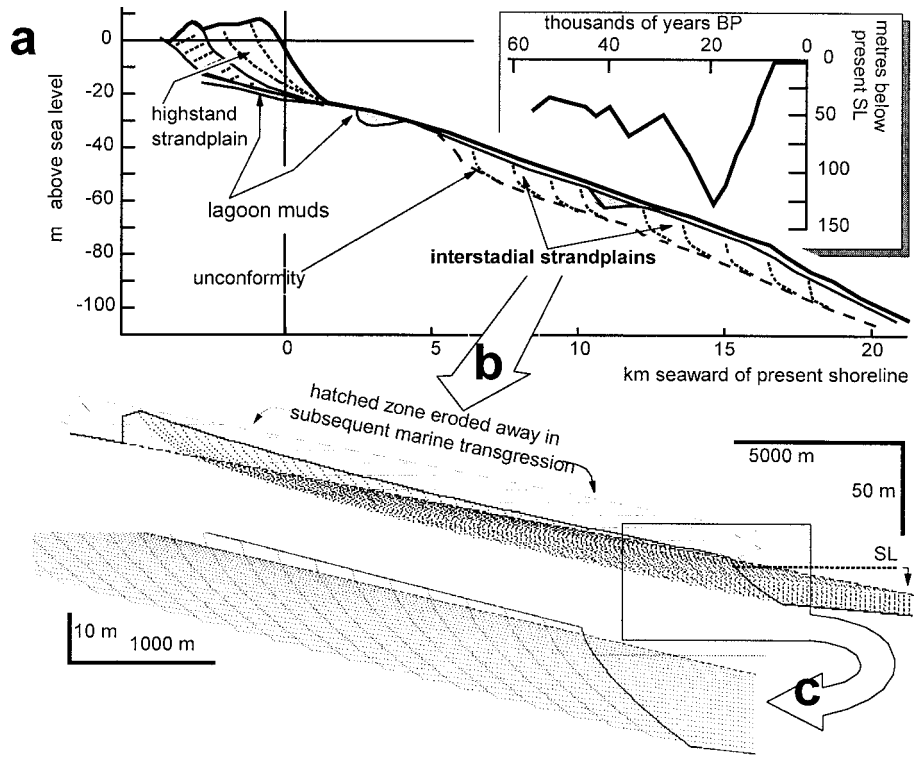

Figure 8. Shoreface response to falling sea level at Tuncurry, SE Australia (Table 3): a) data-model, including strandplains and the sea-level curve (inset); b) STM simulation of strandplain formation; and c) detail of prograding upper shoreface, in which the dotted sub-horizontal lines represent previous erosion surfaces of the lower shoreface when falling sea level was higher, and the dotted steeply dipping curved lines are the buried depositional surfaces of the prograding shoreface.

the STM). This distance was estimated from the extent of the corresponding zone identified under present conditions (simulated in Figure 6). Lowering was achieved by adjusting h_*. Stratigraphic evidence suggests the upper part of the strandplain has been removed in the subsequent Holocene marine transgression and current period of sea-level stillstand (COWELL *et al.*, 1995; ROY *et al.*, 1997). Overall, the process caused a massive reworking of the pre-existing substrate to a depth roughly equivalent to upper-shoreface closure depth (as defined for the decade to century time scale).

Low-Order Backbarrier Processes

Dynamics

The backbarrier component of the coastal tract includes the sub-aerial beach, dunes and lagoon/estuary or coastal lowland equivalent, if present (*cf.* zones A,B,C in Figure 1, Part 1). The backshore can be ignored for the very long times scales (10^4–10^6 years) relevant to the basin-fill problem in exploration geology. Then, transgressive and regressive surfaces in seismic records signify the gross behavior of the continental shelf in response to large (tectono- and glacio-eustatic) sea-level changes and variations in sediment supply (CAREY *et al.*, 1999). Ignoring the backbarrier even on these geological time scales however, requires the simplifying assumption that deposits in lagoons and estuaries can be aggregated into a generalized backstepping coastal sediment wedge during periods of rising sea level. Similarly, but at the other extreme, analysis of short-term coastal change (*e.g.,* dune-erosion models) also can ignore explicit linkages with the backbarrier. These effects are usually represented implicitly in models on intermediate scales (HANSON *et al.*, 2003, this volume), as boundary conditions (Part 1).

A more complete account of coastal behavior however, must include shoreface-backbarrier coupling (Figure 2 in Part 1). For example, in environments with continental-shelf slopes typical of the Columbia and Tuncurry sites, if the backbarrier accommodation space generated by sea-level rise is occupied fully by deposition of fine sediments, then the rates of coastal recession (transgression) can be almost 50 percent less than in the absence of fine sediments. On the other hand, a doubling in the rate of sand bypassing from the shoreface to the backbarrier can increase recession rates by up to 40 percent (Figure 9). Generally, rates of fine-sediment deposition in the lagoon depend on the availability of such sediments from fluvial sources, or from muds mobilized through shoreface erosion. Biogenic sediment production may add to backbarrier sedimentation.

Transfer of sand from the shoreface to the backbarrier driven by sea-level rise causes *barrier rollover* (LEATHERMAN, 1983), a process represented analytically by the Generalized Bruun Rule (DEAN and MAURMEYER, 1983). Barrier rollover

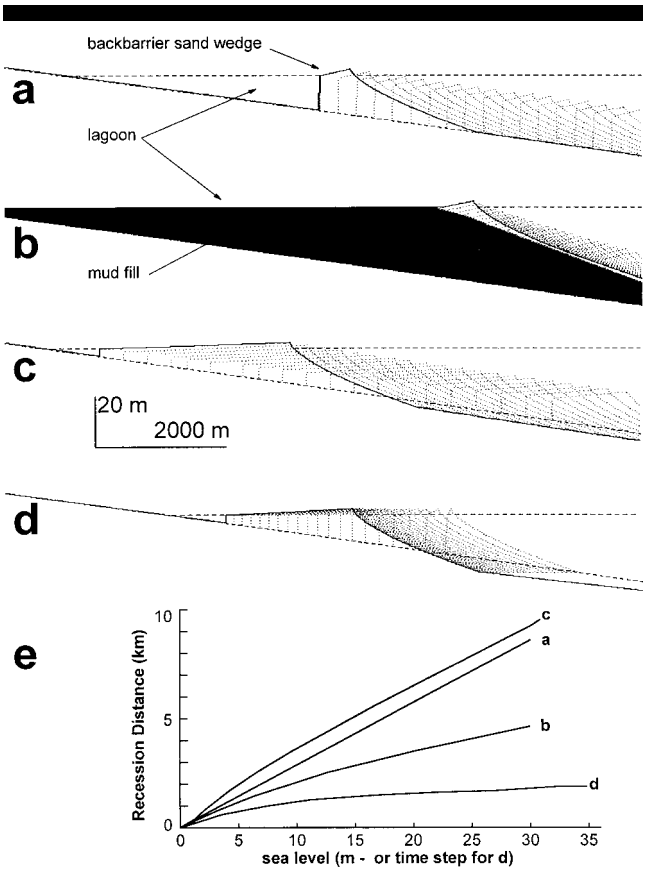

Figure 9. Dependence of shoreface-recession on backbarrier behavior for idealised conditions on a 0.2 degree shelf slope: a) simple barrier rollover with time-invariant backbarrier sand wedge; b) mud deposited at the same rate as sea-level rise; c) width of backbarrier sand wedge increasing with time; d) increasing width of backbarrier sand wedge with constant sea level; and f) comparison of shoreface recession distances in a to d. A sea level rise of 1 m per time step applies to a, b, and c. Sea level is constant in d. All other conditions not specified are the same in each case.

involves bypassing of sediments from the shoreface to the backbarrier (Figure 9a) through washover, tidal-inlet, and transgressive-dune processes (third-order processes in the coastal-tract cascade). Conceptually, the Generalized Bruun Rule aggregates all these processes, simply by assuming that they collectively cause a given rate of sediment bypassing. In the special case analyzed by Dean and Maurmeyer, this is the rate that permits the barrier to maintain a constant form during transgression (in an alongshore spatially averaged sense).

Generally, tidal-inlet processes dominate sediment exchanges between the shoreface and the backbarrier, even in areas where these processes are episodic: *e.g.,* for microtidal barrier islands (LEATHERMAN, 1983). These processes include an interaction between the upper shoreface, the inlet channels, the channels and shoals on the ebb-tide delta and the tidal flats in the basin (ostensibly the flood-tide delta). These morphological elements operate collectively as a third-order sediment-sharing system within the coastal-tract cascade (Table 1 in Part 1). The interaction is characterized by ASMITA (Table 1) in which each component of the system seeks to maintain a dynamic equilibrium with its hydraulic forcing. Equilibrium is expressed by equations of state that relate gross morphologic parameters (specifically the aggregate volume of the positive or negative relief within each component) to relevant forcing parameters (*e.g.,* tidal range or tidal prism). The equations of state are empirically derived relations: *e.g.,* between tidal deltas and the tidal prism (EYSINK, 1991).

Variations in external forcing (*e.g.,* average tidal range) shift the equilibrium state for any or all of the units. Disturbance to the equilibrium of one unit demands changes in each of the others, since all units share a common total sand volume (at third order). The mutual changes result in an exchange of sediment between the various units until the equilibrium state is re-established. Diffusion processes govern the sediment transport between the units, each of which maintains a time-averaged concentration of mobile (suspended) sediments related to the hydraulic forcing. Disturbances in the overall equilibrium cause adjustments involving net sand transfers between the shoreface and backbarrier. Net transfer to or from the backbarrier causes landward and seaward displacement of the upper shoreface respectively.

In application of ASMITA, an equilibrium system is developed and then perturbed to study the responses of the system components and the interaction between these components. An interesting result emerges from the different response times associated with the various components in the system. Once the system is perturbed a series of interactions develop between the components (inlet, tidal basin, and shoreface) that cannot be predicted based on understanding of the timescale of separate adjustment of individual components to their equilibrium state.

In principle, this third-order behavior is affected also by the interaction between the dynamics of the backbarrier sand wedge (primarily the gross flood-tide delta unit) and the fine-sediment fill (muds). Higher rates of mud deposition decrease the tidal prism; the construction of polders in the lagoon can have the same effect. Similarly, the hydrodynamics of the inlet itself regulates discharge, influx and retention times (flushing rates) of water containing fine suspended sediments.

Shoreface-Backbarrier Coupling

Overall, the rate of sand bypassing from the shoreface to the backbarrier controls the rate of upper-shoreface translation landward, illustrated in Figure 9 for idealised conditions with a shelf slope comparable to Columbia and Tuncurry coastal tracts. This bypassing is controlled by the available sediment accommodation space in the backbarrier, and the rate at which this space is regenerated by any sea-level rise. Thus, if the rate of sand bypassing from the shoreface to the backbarrier remains constant, coastal recession occurs at a uniform rate (Figure 9a). If accommodation space available is reduced through mud deposition, then sand transfer from the shoreface to the backbarrier is reduced, which in turn reduces the rate at which the upper shoreface recedes (Figure 9b). If backbarrier space is available to accommodate growth

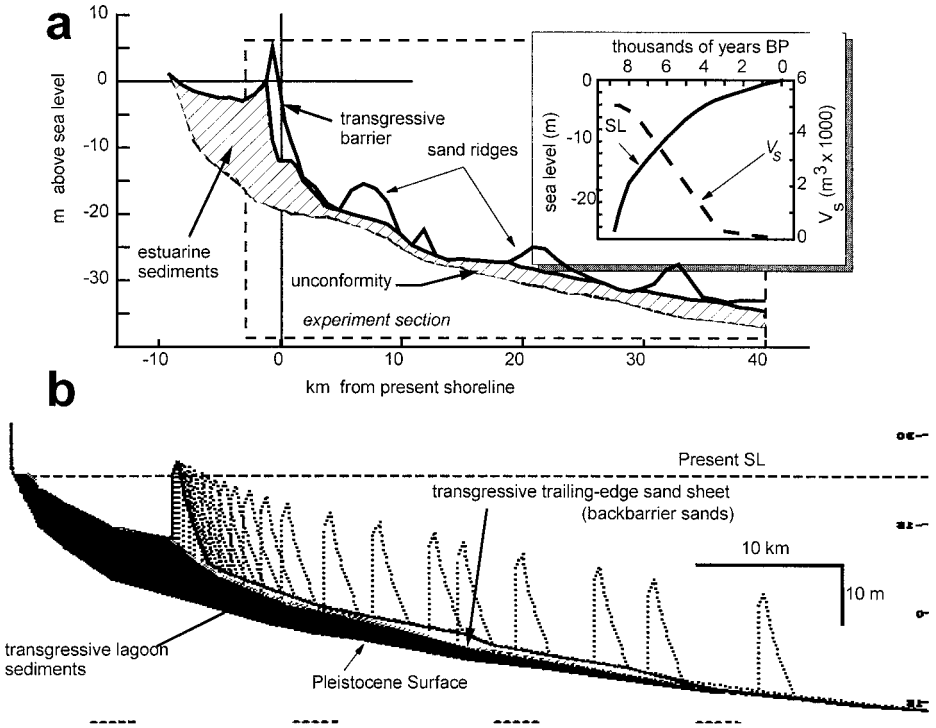

Figure 10. Duck coastal tract, NC USA: a) data-model, and b) STM simulation covering the last 20 m of post-glacial sea-level rise, but before the onset of progradation. Mud deposition was at 30 percent of sea-level increments.

in the backbarrier sand wedge (ostensibly the flood-tide delta), then such growth elevates the rate of shoreface retreat (*cf.,* Figure 9c and 9a) since the upper shoreface and backbarrier sand wedge is a sediment-sharing system. Therefore, even in the absence of sea-level rise, growth of the backbarrier sand wedge occurs at the expense of the shoreface (Figure 9d).

The linear recession of the shoreface for simple barrier rollover across the 0.2° substrate (Figure 9e) occurs at the same rate as inundation would occur over a non-erodable substrate of the same slope. Mud deposition in the lagoon or variations in sand bypassing to the backbarrier cause departures from the inundation rate (b and c in Figure 9e). Despite mud deposition and growth of the tidal delta both occurring at a constant rates (Figure 9b and c), the recession rates in these cases were not constant (Figure 9e). This behavior reflects fundamental non-linearity due to morphological state dependence in coastal evolution (*i.e.,* 'sensitive dependence upon initial conditions'). Although in principle the results of simulations such as those in Figure 9 could be 'interpolated' to decadal time scales for coastal-management purposes, state-dependent effects would need somehow to be taken into account.

E USA: Duck NC. The importance of backbarrier mud deposition in mitigating shoreface retreat is evident for the Duck coastal tract (Figure 10). In this case, the transgressive barrier is so diminutive that the aggregate behavior depends more on the backbarrier than the shoreface itself. The Duck simulation also shows the additional effect of an external littoral supply of sand (V_s in Figure 10a inset). This supply results in the formation of a transgressive sand sheet on the lower shoreface (Figure 10b). This sand sheet blankets the lagoonal muds as they emerge seaward of the receding barrier driven landward by rising sea levels. We assume that this sand sheet was subsequently reworked to form, at least in part, the sand ridges located at present on the lower shoreface (Figure 10a). In reiterative simulations, each with the same sea-level curve, mud deposition was the main controlling variable. Simulated recession (Figure 10b) that gave a final location of the transgressive barrier corresponding to the data-model (Figure 10b) was achieved with mud accretion rates set at 30 percent of sea-level increments.

Central Netherlands: Haarlem. Simulations suggest that the early Holocene evolution of the Holland coastal tract (7000–5800 BP) was entirely regulated by coupling between the upper shoreface and the backbarrier (Figure 11). The coupling involved regulation of backbarrier accommodation space by variations in dimensions of the upper shoreface. Our concepts on this coupling are illustrated further through the following assumptions used to develop the data-model.

1. A progressive increase occurred in depth and width of the shoreface during the post-glacial sea-level rise (Figure 11 inset).
2. The transgressive backbarrier and shoreface formed an amorphous sediment wedge of low relief before about 6000 BP when flows and sediment transfers from the shoreface to the backbarrier were unimpeded because the barrier was poorly developed.

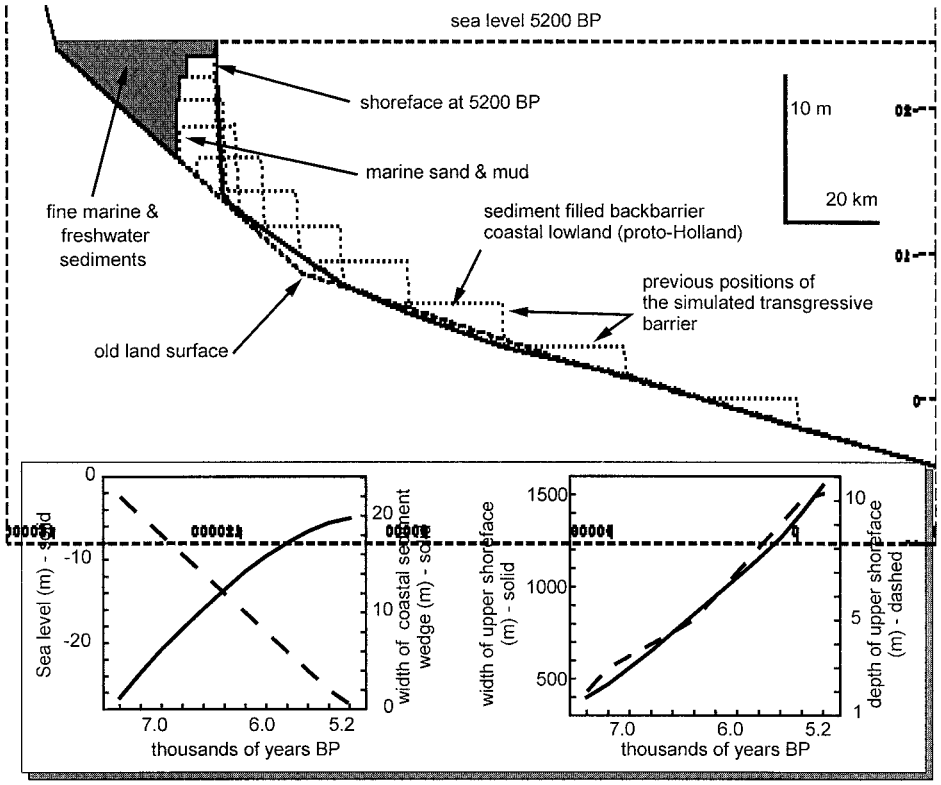

Figure 11. STM simulation of early Holocene evolution of the Holland *coastal tract* driven by post-glacial sea level rise. The insets show time-dependent changes in variables estimated in the *data-model*; Figure 5a gives the *data-model* morphology.

3. Both fine and coarse sediment fractions were conserved when re-exhumed by shoreface retreat: sediments were simply re-incorporated into the backbarrier further landward.
4. The backbarrier filled completely with sediment as fast as new accommodation space was created by the rising sea level.
5. The time-averaged littoral sediment supply was bypassed to the backbarrier at $V_s = 66$ m^{3}a^{-1} during the transgressive phase of Holocene evolution (8.0–5.8 ka BP).
6. Sediment transfers between backbarrier and shoreface became increasingly impeded and subject to normal inlet and overwash processes after about 6000 BP.
7. Shoreface-connected ridges (VAN DE MEENE, 1994) can be ignored in first-order tract behavior because they are higher order features.

Assumption 1 reflects the increasing fetch, water depth and hence wave energy, as the North Sea gradually flooded after the last glacial maximum. We adopted this assumption based on fetch- and depth-limited hindcasting of waves in a North Sea of reduced area: *i.e.,* when the basin first began to flood some 8–7000 years BP. Greater frictional attenuation than at present also can be inferred given that bed gradients were less (*c.* 0.01°) before hydro-isostatic subsidence ensued due to flooding of the basin (LAMBECK, 1995). We justify the second assumption through a) field evidence from exposures of late transgressive deposits (CLEVERINGA, 2000), and b) our interpretation of early conditions when the wave climate (Assumption 1) was probably subordinate to meteorological and astronomical tides.

Assumptions 3 and 4 stem from Assumptions 1 and 2; but they are based also on field data that indicate that the provenance of both coarse and fine sediments was largely the North Sea, with recycling through the backbarrier during rapid marine transgression between 8.0 and 5.8 ka BP (BEETS, *et al.*, 1992, 1995). In reality, sandier sediments occur in the seaward end of the transgressive wedge, while the fine fraction was trapped in the landward extremities of the tidal basin, with freshwater sediments and peat occurring along the mainland shoreline (VAN DER SPEK, 1994).

The sediment supply rate (Assumption 5) was estimated from the total Holocene sediment volume contained within the coastal lowlands of the Holland tract at present. This estimate ($V_s = 66$ m^{3}a^{-1}) is more than double the rate ($V_s = 30$ m^{3}a^{-1}) estimated for the period 5.8 to 2.0 ka BP when the coast was prograding (BEETS *et al.*, 1992): we applied the latter rate to the simulation shown in Figure 5. The higher rate of supply in the early Holocene assumes that 36 m^{3}a^{-1} of fine sediments were included in the total sediment feed from littoral sources sequestered by the backbarrier. Obviously, the fine fraction was not incorporated into the depositional volume during the later shoreface-progradation

phase because the flows on the shoreface were too energetic to permit deposition of fine sediments. The pre-existing floor of the North Sea (including lowstand floodplain and deltaic deposits of the Rhine), and erosional-retreat of promontories to the north and especially the south of the tract provided the source of coarse and fine sediments for the Holland tract during the transgression (BEETS *et al.*, 1992, 1995).

Assumption 6 reflects a decreasing capacity for bypassing of shoreface sediments to the backbarrier as inlets became choked and dune development restricted the occurrence of washover. Such changes in conditions are evident in geological data and are attributed to reduced accommodation space (decreasing rate of sea-level rise) relative to the sediment supply volume (BEETS, *et al.*, 1992, 1995).

Geometric parameters were manipulated in the STM in accordance with these assumptions. Fine and coarse fractions were treated as an undifferentiated barrier-backbarrier sediment wedge in the simulation of early Holocene transgressive phase: *i.e.,* transgressive deposits landward of the shoreface (washover, flood-tide delta, estuarine basin, fluvial-delta and marsh sediments) were lumped together. We simulated this coastal-lowland sediment wedge by maintaining backbarrier width in the STM at values much greater than the lagoon width (Figure 11). During later phases, the effects of Assumption 6 were introduced by applying a progressive reduction in barrier width (Figure 11 inset).

Application of a progressive increase in shoreface dimensions (Assumption 1) caused the simulated elevation and width of the modeled backbarrier to grow through time, and thus also the volume of sediment sequestered by it (Figure 11). Although sediments probably were also mined from the lower shoreface during the transgression (BEETS *et al.*, 1992), in the manner illustrated by Figure 9c, rates of shoreface growth and external sediment feed used in simulations were sufficient to prevent the occurrence of much substrate erosion (Figure 11). Finding evidence for such erosion on the present lower shoreface is problematic because of the amount of modern reworking. Overall, the simulated interplay between shoreface behavior and the sequestering of sediments into the backbarrier resulted in translation of the upper shoreface to within 1200 m of the 5800 BP shoreface location in the data-model (or less than 1.5% of a potential translation distance exceeding 80 000 m).

The simulated reduction in rate of sand bypassing to the backbarrier, with continued littoral sand supply from outside the tract, caused the modeled evolution to flip spontaneously from transgression to regression at 5200 BP (Figure 11). This fundamental change from coastal recession to progradation, despite continued sea-level rise (albeit at a declining rate), was induced entirely through reduction in this sand bypassing.

N Netherlands: Wadden Islands. The first-order coupling of the shoreface and backbarrier is regulated by second-order processes that govern the rate of sand bypassing between the two complexes. This cascade relationship can be represented, for example, by nesting ASMITA within the ADM, STM or HPM (Table 1). Thus, ASMITA computations for the shoreface-backbarrier sediment exchanges were inserted for the sediment-budget in the landward-most grid cell of the ADM. The sink term on the inner shoreface (s_x in equation 7), defined as the region interacting directly with the backbarrier (computational grid cell, $x = X_1$), becomes

$$s_{X_1} = s_b/L_y \tag{8}$$

where s_b is the source/sink term for shoreface-backbarrier sediment exchanges and L_y is the length of coastline represented by the coastal tract. Figure 12 illustrates results of the ADM-ASMITA hybrid model applied to shoreface-backbarrier coupling for the Terschelling barrier island and its Borndiep inlet (The Netherlands Wadden Sea coast, Table 2). The Terschelling-Borndiep data-model assumes that the sediment demand of the Borndiep only affects 20 km (L_y) of the coast up-drift from Terschelling (SHA, 1992). The dimensions of the inlet morphologies are given in Table 4 and the shoreface data-model is shown in Figure 12b.

The simulation involved a sea-level rise of 0.002 m a^{-1} for 200 years, then increasing to 0.004 m a^{-1} for a further 300 years. We assume that, during this period, the inlet morphologies maintain constant surface areas and that there is no net littoral sediment feed. Under these conditions, the rising sea level creates a sediment demand in the Borndiep tidal basin which causes the evolution of the tidal inlet morphologies shown in Figure 12a. In the first 200 years all units are close to their equilibrium states. After the increase in sea-level rise, all units evolve toward new equilibrium volumes, and the sediment sink (s_b) doubles from 0.6 million m^3 a^{-1} to a peak of 1.1 m^3 a^{-1} after 500 years. Simulations were undertaken with and without the inlet (Figure 12b). The comparison shows that inlet behavior predicted by ASMITA has significant consequences for shoreface behavior as the effects feed through the ADM. With the inlet, onshore directed advective transport in the ADM causes erosion of the shoreface beyond water depths of 7 m. Without the inlet, sediment eroded from the upper shoreface is transported further offshore.

The deepening of the shoreface is greatest furthest inshore (Figure 12b). This occurs because, for the hybrid-nesting scheme applied here, the sediment demand of the tidal basin directly affects only the first wet element (X_1) of the ADM. The ADM grid size in this example is about 1000 m. In reality however, significant direct influence of the ebb-tidal delta extends further from the coast: probably up to several kilometers (~5 km). A larger grid size would better capture the direct inlet effects further offshore, but this would detract from the resolution. Alternatively, the model could be refined by dividing the immediate sediment demand over more grid-cells according to a specified distribution (*e.g.,* linear decrease of sediment demand in offshore direction through several grid cells). Nevertheless, Figure 12 adequately demonstrates the principles of nested processes within the cascade hierarchy.

DISCUSSION: SCALE CONSIDERATIONS IN COASTAL MANAGEMENT

Prediction of Mean-trend Coastal Change

The illustrations of low-order coastal behavior in the previous sections may seem to involve scales of little interest in routine coastal management. However, observations on these

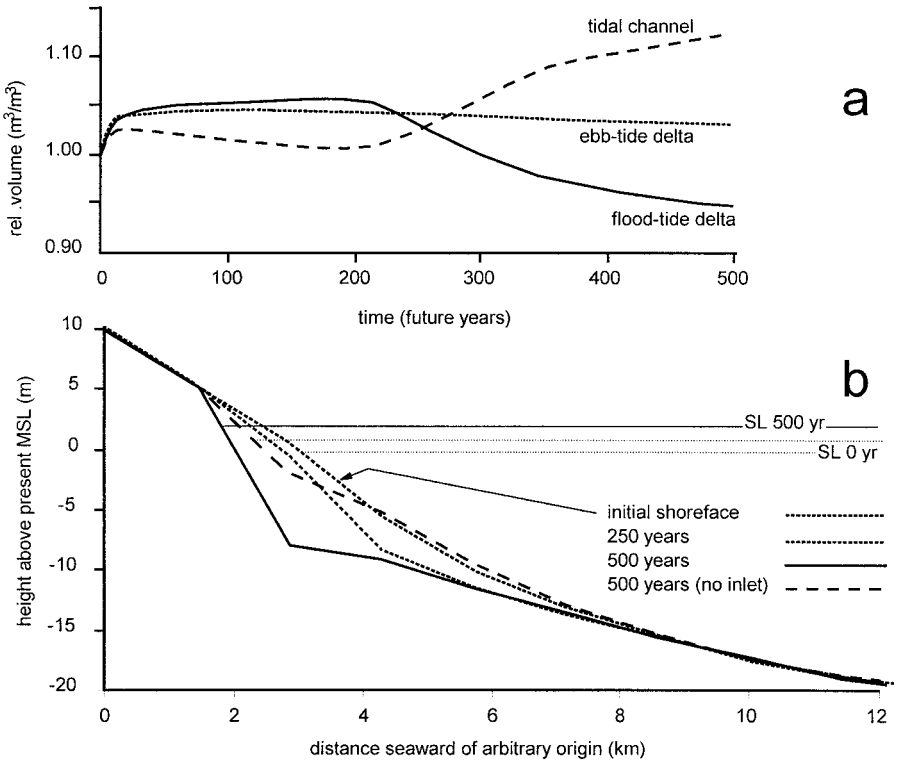

Figure 12. Simulation of coupled shoreface-backbarrier for the barrier island Terschelling and its Borndiep tidal inlet, on The Netherlands Wadden Sea coast, using a hybrid ADM-ASMITA model (Table 1): a) ASMITA predictions of tract-unit volumes (relative to initial values); b) ADM simulation of shoreface evolution with ASMITA inlet effects embedded (plus one case without inlet for comparison).

large scales are required for the occurrence of sufficient change and spatial coverage to resolve the modes, trends and rates in low-order behavior. Once resolved, these trends can be scaled down: from millennia to years if necessary. Thus, provided that the simulation has been wound up numerically to its operational state, the quantitative output over small time steps (years to decades) remain of immediate relevance to core decision making in coastal management, especially where discrimination between chronic and acute coastal erosion is concerned.

From what we know of the problems of up-scaling, coastal-management based on down-scaled predictions can hardly be less valid, even if currently they are less often contemplated. Moreover, downscaling probably provides the more reliable predictions past the decadal time scale. Whereas upscaled predictions can make little use of field data of direct relevance to these time scales, the modeling described above can exploit geological data. Assimilation of these data into behavior models constrain predictions on the shorter time scales. Data that are especially useful in this regard include stratigraphy derived from acoustic seismic, ground-penetrating radar and coring, especially where time-calibrated through radiometric dating. Predictions from aggregated models however only address probable future states. Aggregation precludes exact predictions for particular future instances (i.e, individual realizations).

Table 3. *Surface areas and equilibrium volumes for elements of Borndiep inlet, The Netherlands (*BIEGEL, 1993).

	Area (m^2)	Equilibrium Volume (m^3)
Flood-tide delta	1.77E + 08	1.24E + 08
Inlet channel	9.87E + 07	3.00E + 08
Ebb-tide delta	2.00E + 07	1.33E + 08

Scale Considerations in Delineation of Upper and Lower Shoreface

The lower shoreface is by far the most extensive region under most circumstances. It covers most of the continental shelf, out to the shelf break. Its character varies geographically, reflecting the evolutionary modes of coastal tracts in contrasting environments (Figure 2). Although the classical definition of the shoreface emphasizes the dominance of surface gravity waves in determining the morphology, the importance of other classes of flow in governing sediment dispersal has been recognized increasingly in recent years (NIEDORODA and SWIFT, 1991; WRIGHT, 1995). Recognition of the wide range of sedimentary processes operating on shorefaces has served to blur the offshore demarcation of the shoreface so much that generally it is possible only to trace the process continuum out to the shelf break (*e.g.,* NIEDORODA *et al.*,

1995). The continental-shelf slope is included in the coastal-tract concept since it is in principle also part of this deterministic process continuum. The slope is a region where the effects of gravity become the dominant transport agent. In reality, the process continuum manifested by active sedimentation probably extends onto the shelf slope only under conditions involving high levels of fine sediment input at the coast, where the shelf is narrow, or during sea-level low stands.

The upper shoreface contains the surf zone and extends some distance seaward of it. This distance is time-scale dependent since the upper shoreface is defined as the zone in which detectable changes in bed elevation can occur during a specified period. That is, adjustment of the upper shoreface in response to varying input forcing can be assumed to occur instantaneously for practical prediction of low-order change: *e.g.,* over a single time-step used in large-scale models of the shoreface (STIVE and DE VRIEND, 1995). The morphological time scale, shown schematically in Figure 3 of Part 1 can be estimated directly from field measurements of profile closure, the most commonly applied version of which is the annual closure depth (HALLERMEIER, 1981). Closure depths generally increase with the time period over which observations are made (NICHOLLS *et al.*, 1998; HINTON *et al.*, 1999), so the extent of the upper shoreface increases with time scale (and thus the time step used in a model).

Short-term (*e.g.,* annual) closure depths discriminate the seaward limit to morphological change occurring at the sub-time step level in models of low-order coastal behavior. This seaward limit (*i.e.,* h_* and L_* in eq. 5) and the shoreline circumscribe the *active zone* defined by STIVE and DE VRIEND (1995). Since the active-zone closure depth increases with time scale, longer time steps can be used in modeling longer evolutionary sequences, but only to a limited degree. Low-order coastal change is characterized by significant morphologic change on the lower shoreface (Figure 2 and 3 in Part 1), as shown by the illustrations in the previous section. For low-order coastal evolution therefore, closure provides a measurable index for the time scale of morphological coupling between the upper and lower shoreface. Extrapolation of this index for time spans beyond several decades is the only empirical approach available at present, given the limited temporal coverage in existing data sets for the lower shoreface.

On medium scales, closure is typically observed near the seaward limit of the active zone influenced by breaking waves. The repeated onshore and offshore migration of bars produce large gross fluxes of sediment and a distinct associated closure. At longer time scales, closure can decouple from the active zone and move onto the middle/lower shoreface. Preliminary analysis with the ADM suggests that closure steadily moves offshore with increasing time scale and the primary control shifts from breaking waves to shoaling waves and more general shoreface processes. Repetitive profile observations (since 1965) on the Holland coast to 16 m depths show similar behavior, together with a shoreward closure related to breaking waves (HINTON and NICHOLLS, 1998; HINTON *et al.*, 1999). On half the profiles at a 25-year time scale, the shoreward closure is followed by reopening of the profile on the middle shoreface and a final seaward closure near the limit of the data (about 16 m water depth). Reopening was associated with slow, near-continuous profile erosion: the eroded sand is inferred to move onshore to the active zone (STIVE *et al.*, 1991). The temporal pattern of reopening is nearly linear: extrapolation suggests that in about 50 years, all the profiles on the Holland coast will show reopening, and in about 100 years, all the profiles will be morphodynamically active across the entire surveyed profile.

Process measurements along the US East Coast (NIEDORODA *et al.*, 1985; WRIGHT *et al.*, 1991; 1995; BEAVERS *et al.*, 1999) and in Spain (GARCIA *et al.*, 1998) show that the shoreface is so active that, as time scale increases, closure is likely to move further seaward than the depths indicated from bathymetric data available at present (WRIGHT, 1995; NICHOLLS *et al.*, 1998). Furthermore, closure depth concepts has been applied to sandy systems. In using closure as a time-scale index for low-order change further out on the lower shoreface of the more generic coastal tract (*e.g.,* Figure 4), the influence of different sediment grades (*i.e.* sand, silt and clay) must be taken into account.

SUMMARY AND CONCLUSIONS

Low-order coastal evolution involves systematic coastal change upon which all other morphological changes are superimposed. This type of change manifests itself in coastal management as chronic problems such as shoreline migration that may persist for decades to centuries. For coastal management, low-order coastal change is of first order importance because it controls systematic trends in shoreline movement and morphology, and thus also the shift through time in locations impacted by higher-order changes (*e.g.,* responses to individual storms). At any given time (*i.e.,* on the sub-decadal time scale), the rates and magnitudes of higher-order changes dominate community perceptions, because these changes dominate the morphological-response signal in the short term.

Although important (non-negligible) on the decadal time scale, study of lower-order change requires a longer view to gain resolution (*i.e.,* to discriminate it from the high-order variance). Thus, model calibration is best achieved by hindcast comparison with geological signals of coastal change recorded in deposits laid down over centuries to millenia. The results of these studies can be extrapolated down to the decadal time scale to provide low-order trends upon which higher changes (*e.g.,* measured in monitoring programs) are superimposed. Predictions from aggregated models however only address probable future states. Aggregation precludes exact predictions for particular future instances (i.e, realizations).

Quantitative prediction of rates of change and future shoreline positions must contend with the climatology of forcing and resulting sediment-transport regime prevailing at any given site. That is, predictions must capture the residual effects of a very large number of fluctuations in the direction and intensity of sediment transport summed over time spans (decades to millenia) that are typically four to six orders of magnitude longer than individual transport events (hours to days). Generally, transport residuals are smaller than or sim-

Annex. *Estimates are based on: a) for the period 5000 BP to present, analyses of geological data by* BEETS *et al. (1992); and b) for 7400 to 5000 BP on STM simulations using a sea-level history derived from modeling by* LAMBECK *(1995) involving eustatic and hydro-isostatic effects. Data after 2000 BP are split into sub cells 'south' and 'north' of Haarlem (i.e., Hoek of Holland-Haarlem, and Haarlem-Den Helder respectively).*

						Terms in Coastal-evolution Trajectory (eq. 5)					
Time Calendar Years BP	Rate of Sea-level Rise mm a^{-1}		Shoreline Displacement Advance (+) or Retreat (−) m a^{-1}			$C_p h^*$ m^2 a^{-1}		Accommodation (+/−) Due to Sea-level Change m^3 a^{-1} m^{-1}		Combined Sources: Supply (+) & Loss (−) m^3 a^{-1} m^{-1}	
7400–7200	17.5		−185.3			−1853.2		−8.75		30	
7200–7000	15.5		−132.5			−1324.8		−7.75		30	
7000–6800	14.0		−102.5			−1024.7		−7.00		29	
6800–6600	12.5		−72.8			−728.5		−6.25		29	
6600–6400	12.0		−47.2			−472.4		−6.00		28	
6400–6200	11.5		−37.6			−376.4		−5.75		28	
6200–6000	11.0		−28.2			−282.3		−5.50		27	
6000–5800	9.0		−13.7			−136.8		−4.50		27	
5800–5600	8.0		−0.62			−62.0		−4.00		26	
5600–5400	7.0		−2.4			−24.0		−3.50		26	
5400–5200	5.0		2.6			25.8		−2.50		25	
5150–4500	2.0		2.1			21.0		−1.00		22	
4700–2000	1.0		1.6			16.0		−0.50		17	
2000–1000	0.75 ± 0.25	0.3		−1.7	−17		−17	−0.38	3		−17
1125–375	0.75 ± 0.25	−1.1		−3.9	−31		−39	−0.38	−11		−39
500–150	0.75 ± 0.25	−0.6		−2.7	−27		−27	−0.38	−6		−27
150–0	1.75 ± 0.25	0.45		−1.65	−16		−17	−0.38	5		−16.5
Sub-cell:		south		north	south		north		south		north

ilar to the predictive error for gross transport based on standard methods. Thus, scaling up estimates of the residuals to quantify the transport regime associated with the forcing climatology is unlikely to provide reliable predictions (DE VRIEND, 2003, this volume).

We attempt to sidestep this problem through a behavior-oriented approach in modeling low-order coastal change. This approach deals with the forcing climatology directly through a highly aggregated representation of the processes. We have developed three types of behavior models that capture forcing climatology in different ways: *i.e.,* as macroscopic forcing, summary forcing and abbreviated forcing. We applied these models in comparative experiments on long-term coastal change using data sets from the contrasting environments of SE Australia, Pacific and Atlantic USA, and European North Sea Coasts (Netherlands).

Data-models were compiled for each data set to define coastal tracts with spatial and process dimensions consistent with the behavior models applied, and to discriminate between boundary conditions and internal components. The internal components of the tract interact by sharing a common pool of sediments. The data-templating procedures for developing the data-models consume about 90 percent of the modeling effort: the numerical experiments are a minor component of the work overall. The level of expertise required for data-model templating makes these types of models unsuitable as coastal-management tools for use by novices.

We assumed alongshore homogeneity in morphology and processes for each data set when compiling data-models. Thus, each coastal cell was represented (through alongshore averaging) as a cross-shore profile of unit width. The experiments then entailed comparison of simulated coastal-change against coastal evolutions evident in the data-models. Synthesis of the modeling results demonstrates the following coastal-tract principles:

- The gross kinematics of the coastal tract are constrained and steered by sediment-mass continuity. The rate of coastal advance or retreat is determined quantitatively by the balance between the sediment accommodation-space generated due to sea-level rise (or lost due to sea-level fall), and sediment availability (being the sum of external sinks and sources). The relative sea-level change is a virtual sink/source term since there is no absolute loss, although the response is comparable to the impact of a real source/sink regarding horizontal movements of the upper shoreface.
- The upper and lower shoreface are coupled in first-order coastal change. Sediments (particularly the fine fraction) diffuse from the upper out across the lower shoreface (*e.g.,* the US Columbia River coast), but if the lower shoreface is shallower than required for equilibrium, then sand is transferred to the upper shoreface from the landward portion of the lower shoreface. This transfer offsets coastal-recession tendencies caused by other factors (*e.g.,* the central Netherlands coast) or, in the absence of these, the transfer produces a seaward advance of the coast (*e.g.,* the Tuncurry coast in SE Australia), and during periods of falling sea level.
- The upper shoreface and backbarrier (lagoon, estuary or mainland) are coupled in first-order coastal change. Sediment accommodation-space is generated in the backbarrier by sea-level rise (and reduced by sea-level fall), but the amount of space is moderated also by influx of fine sediments from the coast, or sand and mud from fluvial and biogenic sources. Remaining space can then be occupied by

sand transferred from the upper shoreface causing a retreat of the latter: *e.g.,* transgressive phases of the central Netherlands coast and the US-Atlantic (Duck) coast during the mid Holocene, and the Netherlands Wadden Sea coast under present conditions. Conversely, an increase in the tidal prism of active tidal basins (due to changes in tidal forcing) causes a transfer of sand from the backbarrier to the shoreface causing seaward advance of the latter.

- Rates of first-order coastal evolution due to upper-shoreface couplings with the backbarrier and lower shoreface are governed by a) second-order processes of the latter two sub systems, and b) the zero-order forcings of relative sea-level change and rates of external sediment supply or loss to the coastal tract.

ACKNOWLEDGMENTS

This study contributes toward the PACE project under the European Union Marine Science and Technology program (MAST-III contract MAS3-CT95-0002) with additional funding from Australian National Greenhouse Advisory Committee. Collaboration was funded by grants from Australian Department of Industry Science and Technology and the Netherlands Research Organization (NWO). Preparation the datamodel for Duck, NC, USA was undertaken in collaboration with the Virginia Institute of Marine Science.

LITERATURE CITED

ATWATER, B.F.; NELSON, A.R.; CLAGUE, J.J.; CARVER, G.A.; YAMAGUCHI, D.K.; BOBROWSY, P.T.; BOURGEOIS, J.; DARIENZO, M.E.; GRANT, W.C.; HEMPHILL-HALEY, E.; KELSEY, M.H.; JACOBY, G.C.; NICHENKO, S.P.; PALMER, S.P.; PETERSON, C.D. and REINHART, M.A., 1995. Summary of coastal geological evidence for past great earthquakes at the Cascadia subduction zone. *Earthquake Spectra,* 11, 1–18.

BEAVERS, R.; HOWD, P.; BIRKEMEIER, W. and HATHAWAY, K., 1999. Evaluating profile data and depth of closure with solar altimetry. *Proceedings of Coastal Sediments '99,* American Society of Civil Engineers, 479–490.

BEETS, D.J.; VAN DER VALK, L., and STIVE, M.J.F., 1992. Holocene evolution of the coast of Holland. *Marine Geology,* 103, 423–443.

BEETS, D.J.; CLEVERINGA, P.; LABAN, C. and BATTEGAZORE, P., 1995. Evolution of the lower shoreface of the coast of Holland between Monster and Noordwijk. *Netherlands Royal Geological Service Bulletin,* 52, 235–247.

BIEGEL, E.J., 1993. *Morphological changes due to sea-level rise in tidal basins in the Dutch Wadden Sea versus concepts morphological response model MORRES.* Report IMAU-93.14. Utrecht University: Institute for Marine and Atmospheric Research Utrecht, 57 p.

BOWEN, A.J., 1980. Simple models of nearshore sedimentation, beach profiles and longshore bars. *In*: MCCANN, S.B. (ed.), *The Coastline of Canada,* Geological Survey of Canada Paper, 80–10, 1–11.

BRUUN, P., 1962. Sea-level rise as a cause of shore erosion. *Journal of Waterways Harbors Division,* American Society of Civil Engineers, 88, 117–130.

BUIJSMAN, M.C., 1997. *The impact of gas extraction and sea-level rise on the morphology of the Wadden Sea.* Report H3099.30, Delft Hydraulics, Delft, 78p.

CAREY, J. S.; SWIFT, D. J. P.; STECKLER, M.; REED; C. W. and NIEDORODA, A. W., 1999. High resolution sequence Stratigraphy modeling: effects of sedimentation processes. *Society of Economic Palaeontologists and Mineralogists Special Publication* 62, 151–164.

CHAPPELL, J. and POLACH, H., 1991. Post-glacial sea-level rise from a coral record at Huon Peninsula, Papua New Guinea. *Nature,* 349, 147–49.

CLEVERINGA, J., 2000. *Reconstruction and modelling of Holocene coastal evolution of the western Netherlands.* University of Utrecht: Geologica Ultraiectina, No. 200, 197p.

COWELL, P.J.; HANSLOW, D.J. and MELEO, J.F., 1999a. The Shoreface. *In*: SHORT, A.D. (ed.), *Handbook of Beach and Shoreface Morphodynamics.* Chichester: Wiley, 37–71.

COWELL, P.J.; ROY, P.S.; CLEVERINGA, J., and DE BOER, P.L., 1999b. Simulating coastal systems tracts using the shoreface translation model. *Society of Economic Palaeontologists and Mineralogists Special Publication,* 62, 165–175.

COWELL, P.J.; ROY, P.S. and JONES, R.A., 1995. Simulation of LSCB using a Morphological Behaviour Model. *Marine Geology,* 126, 45–61.

COWELL, P.J.; STIVE, M.J.F.; NIEDORODA, A.W.; DE VRIEND, H.J.; SWIFT, D.J.P.; KAMINSKY, G.M., and CAPOBIANCO, M., 2003. The Coastal-Tract (Part 1): A conceptual approach to aggregated modelling of low-order coastal change. *Journal of Coastal Research* (this volume)

COWELL, P.J.; STIVE, M.J.F.; ROY, P.S.; KAMINSKY, G.M.; BUIJSMAN, M. C.; THOM, B.G. and WRIGHT, L.D, 2001. Shoreface Sand Supply to Beaches. *Proceedings of the 27th International Conference on Coastal Engineering,* American Society of Civil Engineers, 2495–2508.

CURRAY, J.R., 1964. Transgressions and regressions. *In*: MILLER, R.C. (ed.), *Papers in Marine Geology,* New York: McMillan, 175–203.

DEAN, R.G., 1991. Equilibrium beach profiles: characteristics and applications. *Journal of Coastal Research,* 7, 53–84.

DEAN, R.G. and MAURMEYER, E.M., 1983. Models of beach profile response. *In*: Komar, P. and Moore, J. (eds), *CRC Handbook of Coastal Processes and Erosion,* Boca Raton: CRC Press, 151–165.

DE VRIEND, H.J.; CAPOBIANCO, M.; CHESTER, T.; DE SWART, H.E.; LATTEUX, B. and STIVE, M.J.F., 1993. Approaches to long-term modelling of coastal morphology: a review. *Coastal Engineering,* 21, 225–269.

EYSINK, W.D., 1991. Morphologic response of tidal basins to changes. *Proceedings of the 21st International Conference on Coastal Engineering,* American Society of Civil Engineers, 1948–1961.

FIELD, M.E.; MEISBURGER, E.P.; STANLEY E.A. and WILLIAMS, S.J., 1979. Upper Quaternary peat deposits on the Atlantic inner shelf of the United States. *Geological Society of America Bulletin,* New York, 90, 618–628.

GARCIA, V.; JIMENEZ, J.A.; SANCHEZ-ARCILLA, A.; GUILLEN, J. and PALANQUES, A., 1998. Short-term relatively deep sedimentation on the Ebro Delta coast: Opening the closure depth. *Proceedings of the 26th International Conference on Coastal Engineering,* American Society of Civil Engineers, 2902–2912.

HALLERMEIER, R.J., 1981. A profile zonation for seasonal sand beaches from wave climate, *Coastal Engineering,* 4, 253–277.

HINTON, C. and NICHOLLS, R.J. 1998. Depth of closure along the Holland coast. *Proceedings 26th International Conference on Coastal Engineering,* American Society of Civil Engineers, 2913–2925.

HINTON, C.; NICHOLLS, R.J. AND DUNSBERGEN, D. 1999. Profile Re-Opening on the Shoreface of the Holland Coast. *Proceedings Coastal Sediments '99,* American Society of Civil Engineers, 535–550.

KAMINSKY, G.M.; RUGGIERO, P.; GELFENBAUM, G. and PETERSON, C., 1997. Long term coastal evolution and regional dynamics of a US Pacific Northwest littoral cell. *Proceedings of Coastal Dynamics '97,* American Society of Civil Engineers, 614–623.

LAMBECK, K., 1995. Late Devensian and Holocene shorelines of the British Isles and North Sea from models of glacio-hydro-isostatic rebound. *Journal of the Geological Society,* 152, 437–448.

LEATHERMAN, S.P., 1983. Barrier dynamics and landward migration with Holocene sea-level rise. *Nature,* London, 301, 415–418.

MEISBURGER, E.P.; JUDGE, C., and WILLIAMS, S.J., 1989. Physiographic and geological setting of the Coastal Engineering Research Centre's field research facility. Washington, *US Army Corp of Engineers, Miscellaneous Paper CERC,* 89-9, 28 p.

MEYERS, R.A.; SMITH, D.G.; JOL, H.M. and PETERSON, C.D. 1996. Evidence for eight great earthquake-subsidence events detected

with ground penetrating radar, Willapa barrier, Washington. *Geology,* 24, 99–102.

NICHOLLS, R.J.; BIRKEMEIER, W.A. and LEE, G-H., 1998. Evaluation of depth of closure using data from Duck, NC, USA. *Marine Geology,* 148, 179–201.

NIEDORODA, A.W. and SWIFT, D.J.P., 1991. Shoreface processes. *In*: HERBICH, J.B. (ed.), *Handbook of Coastal and Ocean Engineering,* Vol. 2, Houston: Gulf Publishing Co., 736–769.

NIEDORODA, A.W; REED, C.W.; SWIFT, D.J.P., ARATO, H. and HOYANAGI, K., 1995. Modeling shore-normal large-scale coastal evolution. *Marine Geology,* 126, 1/4, 181–200.

PETERSON C. and PHIPPS J. B., 1992. Holocene sedimentary framework of Grays Harbor basin, Washington, USA. *SEPM Special Publication No.48,* Society for Sedimentary Geology, 237–285.

PILKEY, O.H.; YOUNG, R.S.; RIGGS, S.R.; SMITH, A.W.; WU, H. AND PILKEY, W.D., 1993. The concept of shoreface profile equilibrium: A critical review. *Journal of Coastal Research,* 9, 255–278.

REED, C.W.; NIEDORODA, A. and SWIFT, D.J.P., 1999. Modeling sediment entrainment and transport processes limited by bed armoring. *Marine Geology,* 154, 143–154.

ROY, P.S.; COWELL, P.J.; FERLAND, M.A. and THOM, B.G., 1994. Wave dominated coasts. *In:* CARTER, R.W.G. and WOODROFFE, C.D. (eds), *Coastal Evolution: Late Quaternary shoreline morphodynamics,* Cambridge: Cambridge University Press, 121–186.

ROY, P.S.; ZHUANG, W-Y; BIRCH, G.F.; COWELL, P.J. and COGXIZN LI, 1997, *Quaternary Geology of the Forster-Tuncurry coast and shelf, southeast Australia.* Geological Survey Report: GS 1992/201, Sydney: NSW Dept. of Mineral Resources, 405p.

SHA, L. P., 1992. *Geological research in the Ebb-tidal delta of the 'Het Friesche Zeegat', Wadden Sea, The Netherlands.* Haarlem: Rijks Geologische Dienst, 20p.

SHERWOOD, C.R., 1995. *Measurements and modeling of suspended-sediment transport on the Northern California continental shelf.* PhD dissertation, Seattle: University of Washington, 175p.

SLOSS, L.L., 1962. Stratigraphical models in exploration. *Journal of Sedimentary Petrology,* 32, 415–422.

STERNBERG R.W., 1986. Transport and accumulation of river-derived sedimentation the Washington continental shelf, USA. *Journal of the Geological Society,* London, 143, 945–956.

STIVE, M.J.F. and DE VRIEND, H. J., 1995. Modelling shoreface profile evolution. *Marine Geology,* 126, 235–248.

STIVE, J.F.; CAPOBIANCO, M.; WANG, Z.B.; RUOL, P. and BUIJSMAN, M.C., 1998. Morphodynamics of a tidal lagoon and the adjacent coasts. *In*: DRONKERS, J. and SCHEFFERS, M. (eds), *Physics of estuaries and coastal seas: Proceedings of the 8th International Biennial Conference on Physics of Estuaries and Coastal Seas.* Rotterdam: Balkema, 397–407.

STIVE, M.J.F.; ROELVINK, D.J.A. and DE VRIEND, H.J., 1991. Large-scale coastal evolution concept. *Proceedings 22nd International Conference on Coastal Engineering,* American Society of Civil Engineers, 1962–74.

SWIFT, D.J.P., 1976. Continental shelf sedimentation. *In*: STANLEY, D.J. and SWIFT, D.J.P., (eds.) *Marine Sediment Transport and Environmental Management,* New York: Wiley, 311–350.

THORNE, J.A. and SWIFT, D.J.P., 1991. Sedimentation on continental margins, II: application of the regime concept. *In*: SWIFT, D.J.P.; OERTEL, G.F.; TILLMAN, R.W. and THORNE, J.A. (eds), *Shelf sand and sandstone bodies—Geometry, facies and sequence stratigraphy,* Special Publication No. 14 of the International Association of Sedimentologists, Oxford: Blackwell Scientific Publications, 33–58.

THORNE, J.A.; GRACE, E; SWIFT, D.J.P. and NIEDORODA, A.N., 1991. Sedimentation on continental margins, III: the depositional fabric—an analytical approach to stratification and facies identification. *In*: SWIFT, D.J.P.; OERTEL, G.F.; TILLMAN, R.W. and THORNE, J.A. (eds), *Shelf sand and sandstone bodies—Geometry, facies and sequence stratigraphy,* Special Publication No. 14 of the International Association of Sedimentologists, Oxford: Blackwell Scientific Publications, 59–87.

VAN DE MEENE, J.W.H., 1994. *The Shoreface-Connected Ridges Along the Central Dutch Coast.* Utrecht: Netherlands Geographical Studies 174, 222p.

VAN DER SPEK, A., 1994. *Large-scale Evolution of Holocene Tidal Basins in The Netherlands.* Ph.D. Thesis, Utrecht: University of Utrecht, 191p.

VAN DER VALK, L., 1992. *Mid- and Late-Holocene coastal evolution in the beach-barrier area of the western Netherlands.* Ph.D. thesis, Amsterdam: Vrije Universiteit, 235p.

VAN STRAATEN, L.M.J., 1965. Coastal barrier deposits in south and north Holland—in particular in the area around Scheveningen and Ijmuiden. *Meded. Geol. Sticht.*, NS, 17, 41–75.

WANG, Z.B.; KARSSEN, B.; FOKKINK, R.J. and LANGERAK, A., 1996. A dynamic/empirical model for estuarine morphology. *In*: DRONKERS, J. and SCHEFFERS, M. (eds), *Physics of estuaries and coastal seas: Proceedings of the 8th International Biennial Conference on Physics of Estuaries and Coastal Seas.* Rotterdam: Balkema, 279–286.

WOLF, S. C.; HAMER, M. R. and MCCROY P. A., 1997. *Quaternary Geologic Investigations of the continental shelf offshore southern Washington and northern Oregon.* Open-file report 97–677. U.S. Department of the Interior, U.S. Geological Survey. 4 plates.

WOLMAN, M.G. and MILLER, J.P., 1960. Magnitude and frequency of forces in geomorphic processes. *Journal of Geology,* 68, 54–74.

WRIGHT, L.D., 1995. *Morphodynamics of Inner Continental Shelves.* Boca Raton: CRC Press, 241p.

WRIGHT, L.D.; BOON, J.D.; KIM, S.C. and LIST, J.H., 1991. Modes of cross-shore sediment transport on the shoreface of the Middle Atlantic Bight. *Marine Geology,* 96, 19–51.